Titre: Title:	An investigation of the stress state in inclined backfilled stopes using flac-2D
Auteurs: Authors:	Li Li et Michel Aubertin
Date:	2008
Type:	Rapport / Report
Référence: Citation:	Li, L. & Aubertin, M. (2008). *An investigation of the stress state in inclined backfilled stopes using flac-2D* (Rapport technique n° EPM-RT-2008-01).

EPM–RT–2008-01

AN INVESTIGATION OF THE STRESS STATE IN INCLINED BACKFILLED STOPES USING FLAC-2D

Li Li, Michel Aubertin
Département des génies civil, géologique et des mines
École Polytechnique de Montréal

Mars 2008

EPM-RT-2008-01

AN INVESTIGATION OF THE STRESS STATE IN INCLINED BACKFILLED STOPES USING FLAC-2D

Li LI[1], Michel AUBERTIN[1, 2]

[1]Department of Civil, Geological and Mining Engineering, École Polytechnique de Montréal, C.P. 6079, Succursale Centre-ville, Québec, H3C 3A7, Canada

[2]Industrial NSERC Polytechnique-UQAT Chair on Environment and Mine Wastes Management (http://www.polymtl.ca/enviro-geremi/).

FIRST PUBLISHED AS INTERNAL REPORT: OCTOBER 2007
TECHNICAL REPORT ISSUED: MARCH 2008

Dépôt légal :
Bibliothèque nationale du Québec, 2008
Bibliothèque nationale du Canada, 2008

EPM-RT-2008-01
An investigation of the stress state in inclined backfilled stopes using FLAC-2D
par: Li Li[1], Michel Aubertin[1, 2]

[1]Department of Civil, Geological and Mining Engineering, École Polytechnique de Montréal
[2]Industrial NSERC Polytechnique-UQAT Chair on Environment and Mine Wastes Management

ABSTRACT

Evaluating the stresses in backfilled stopes constitutes a critical step for insuring underground mine safety and production. In recent years, the authors have presented methods to conduct numerical and analytical investigations to assess the stress state in backfilled stopes. The results have shown the existence of arching effects due to the stress transfer along stope walls. To date, most work applies to (sub)vertical openings and only limited studies relate to inclined stopes. In this report, the results of an extensive numerical investigation are presented. Emphasis is placed on the influence of stope geometry and backfill properties, and also on the effect of the filling sequence. Results indicate that arching effects also develop in inclined stopes. The most influential factors on the stress distribution are backfill shear strength parameters (cohesion c' and friction angle ϕ'), Poisson's ratio μ, and dilatation angle ψ'. Some of these not only affect the stress magnitude, but also the distribution pattern which can also be linked to the filling sequence. One of the original outcomes from this study indicates that when increasing the value of c', the mechanical behavior of backfill tends to change from that of a particulate material to that of a consolidated medium, with each layer responding somewhat like a beam to vertical loads. The results are compared to others obtained in previous investigations and discussed in relation to the effect of the influence factors and their implications for the analysis of backfilled stopes.

Key words: Stress analysis; Arching effect; Mining; Backfill; Earth pressures; Stopes; Numerical modeling.

RÉSUMÉ

L'évaluation de contraintes dans un chantier remblayé constitue une étape critique pour assurer la sécurité et la production des mines souterraines. Depuis plusieurs années, les auteurs ont développé des méthodes d'investigation analytiques et numériques pour estimer l'état de contraintes dans les chantiers remblayés. Les résultats ont démontré l'existence d'un effet d'arche dû au transfert des contraintes le long des parois des chantiers. Dans ce rapport, des résultats d'une investigation numérique seront présentés. L'emphase est placée sur l'influence de la géométrie, des propriétés du remblai et de la séquence de remblayage. Les résultats indiquent que l'effet d'arche se développe aussi dans des chantiers inclinés. Les facteurs d'influence les plus significatifs sur la distribution des contraintes sont les paramètres de résistance au cisaillement (cohésion c' et angle de frottement ϕ'), le coefficient de Poisson μ, et l'angle de dilatance ψ'. Certains de ces paramètres affectent non seulement la grandeur des contraintes, mais aussi la forme de la distribution, qui peut également être liée à la séquence de remblayage. Cette étude indique que le comportement mécanique du remblai passe de celui d'un matériau particulaire à celui d'un milieu consolidé, où chaque couche répond comme une poutre en flexion sous charges verticales. Les résultats sont comparés avec d'autres obtenus lors d'investigations précédentes, et discutés en relation avec l'effet des facteurs d'influence et de leur implication pour une analyse des chantiers remblayés.

Mots clés: Analyse de contraintes, Effet d'arche, Mines, Remblayage, Pression de terre, Chantier, Modélisation numérique.

TABLE OF CONTENTS

LIST OF FIGURES

LIST OF TABLES

1. INTRODUCTION

Mine backfill is often used in underground mine excavations to insure safer working conditions. Underground backfilling is also gaining momentum as a mine waste management approach (Aubertin et al. 2002). General overviews on mining with backfill including backfill technology, the mechanical and hydraulic behavior of fill materials, and related environmental issues have been presented by Cowling (1998), Hassani and Archibald (1998), Belem et al. (2002), Aubertin et al. (2005), and Benzaazoua et al. (2005).

As the primary purpose of backfill is to improve ground stability conditions around mine stopes, its in situ mechanical response is a key concern. Studies on backfill properties have shown that these can vary widely, depending on the type and proportion of binder(s) and characteristics of the filler and water. As an example, a typical paste backfill containing 4.5% (w/w) of Portland cement shows a compressive strength in the range of 500 to 600 kPa and an elastic modulus between 200 to 300 MPa (e.g., Belem et al. 2000). These values, which are fairly common for fill materials, indicate that the backfill is "soft" with respect to the mechanical behavior of the surrounding rock mass. This difference in the mechanical properties between the backfill and rock mass tends to induce a stress redistribution in backfilled stopes and surrounding walls (due to the relative displacement along the interfaces). This is particularly the case in relatively narrow stopes, where a load transfer to the stiff abutments can cause an arching effect that leads to a decrease in the vertical stress compared to the overburden pressure (Aubertin 1999; Aubertin et al. 2003; Li et al. 2003, 2005a). This arching effect has been confirmed by in-situ stress measurements (e.g., Knutsson 1981; Hustrulid et al. 1989; Belem et al. 2004; Grabinski et al. 2007) and by laboratory tests (e.g., Mitchell 1992; Pirapakaran and Sivakugan 2007a). Arching has also been observed in other similar structural systems where a relatively soft material (like soil or grain) is placed between stiff abutments; examples include silos and bins (Cowin 1977; Blight 1986; Drescher 1991), ditches (Spangler and Handy 1984), retaining walls (Wang 2000; Take and Valsangkar 2001), and cut-off walls (Filz 1996; Kamon et al. 2006). An important feature of arching is the transfer mechanism which reduces the stress in the backfill, as the vertical loads are redistributed to the stiffer confining walls. Stress increases due to a reverse (negative) arching effect may also occur when the fill is surrounded by a softer material (e.g., McCarthy 1988; Brachman and Krushelnitzky 2005; Kang et al. 2007); this behavior will not be addressed here.

The load distribution resulting from arching can be investigated using physical models, field measurements, analytical solutions, and computational modeling. The latter two approaches are

particularly useful for engineering purposes, as they may be used to investigate the factors influencing stress distribution around openings. In this regard, analytical solutions are known to suffer from significant limitations because of the simplifying assumptions behind their formulation. For instance, most existing analytical solutions are only applicable to (sub-) vertical stopes, in which the response of the backfill material is governed by a perfectly plastic constitutive law based on the Coulomb yield criterion. Analytical solutions typically cannot account for stope wall inclination, wall convergence, excavation sequence, and more elaborate constitutive behavior. Numerical models are much more flexible, and can address the above mentioned factors in stress analysis. There are, however, relatively few examples of numerical models developed for backfilled stopes. Hustrulid et al. (1989) are among those who focused on the response of backfilled stopes, by using a finite element scheme based on linear elasticity theory. They simulated the nonlinear response of a backfilled stope with a piecewise linear elastic law (without a yield criterion), empirically relating the elastic modulus with the mean stress. Aubertin et al. (2003) showed results obtained with the finite element code Phase^2 (from Rocscience) for vertical stopes. Li et al. (2003) relied on the widely used software FLAC (Fast Lagrangian Analysis of Continua), developed by Itasca (2002), to evaluate earth pressures in narrow backfilled sub-vertical stopes, based on a pseudo-dynamic approach. It was found that FLAC is well adapted to assess the stress state in backfilled stopes. More recently, Li et al. (2007) adopted a pseudo-static procedure to investigate the stress distribution in inclined stopes. This modeling procedure consists of considering a single step filling sequence, with the fill initially having a fictitiously high strength. When the backfill mass reaches an equilibrium stress state, the actual material properties are then attributed to the fill and additional calculations are made until the new equilibrium state is reached. Stresses obtained in this manner usually have a continuous distribution in the stopes. Their magnitudes are generally somewhat lower than those obtained with the pseudo-dynamic approach used by Li et al (2003), while they compare well with analytical solutions for idealized (simplified) cases.

In this report, new modeling results obtained with FLAC-2D using a multi-step filling procedure are presented. Stopes with different geometry and backfill properties are simulated. Results illustrate the influence of the various factors. It is also shown that the filling sequence may have a significant effect on the stress state, especially when the fill is dilatant or has a relatively high cohesion. The results obtained here are discussed and compared with those obtained in previous investigations where simplified procedures were used. The numerical results presented here address issues of interest to the mining industry and to other areas of backfill applications.

2. SIMULATIONS WITH FLAC-2D

Backfill, with or without cement, typically has a nonlinear mechanical response. This behavior can be simulated with the well-known code FLAC (Fast Lagrangian Analysis of Continua). FLAC-2D is a two-dimensional finite difference program which uses an explicit, Lagrangian calculation scheme and a mixed-discretization zoning technique. It is well adapted for geotechnical problems consisting of several stages such as sequential excavation and/or backfilling. Various publications illustrate and discuss the main features of this code (e.g., Detournay and Hart 1999; Billaux et al. 2001; Andrieux et al. 2003). A detailed assessment of the stress state in backfilled stopes can readily be obtained with FLAC-2D.

Figure 1 shows a typical inclined backfilled stope. This configuration is used here to assess the effect of various influence factors. The rock mass is considered homogeneous, isotropic and linearly elastic, with the following parameters: E_r = 30 GPa (Young's modulus), μ_r = 0.3 (Poisson's ratio), γ_r = 27 kN/m^3 (unit weight). The backfill obeys an elasto-plastic law with the Coulomb criterion. Its properties are described by the values of E, μ, and γ, with the friction angle ϕ', cohesion c', and dilatation angle ψ'. The stope is filled to a final height of 45 m. The inclination of the stope is given by α (which varies from 90° to 60° with respect to the horizontal). Figure 2 shows the mesh used for numerical modeling performed in this study. It includes 60×180 elements for vertical stopes and 120×180 elements for inclined stopes. Filling is generally performed in four steps (layers) in the simulations. Elastic convergence in the rock mass walls is completed before adding a new layer. The choices of mesh and filling steps are discussed near the end of the paper. Table 1 presents details of the simulations performed, with the specific conditions and properties used, together with the corresponding figures.

3. STRESS ANALYSES

The numerical calculations are used to investigate the influence of various parameters on the stress distribution. The authors present a series of results that illustrate the effect of wall inclination (α) and stope width (B), backfill modulus (E), Poisson's ratio (μ), internal friction angle (ϕ'), cohesion (c'), and dilatation angle (ψ') (see Table 1 for details).

Figure 1. The reference case for the inclined backfilled stope.

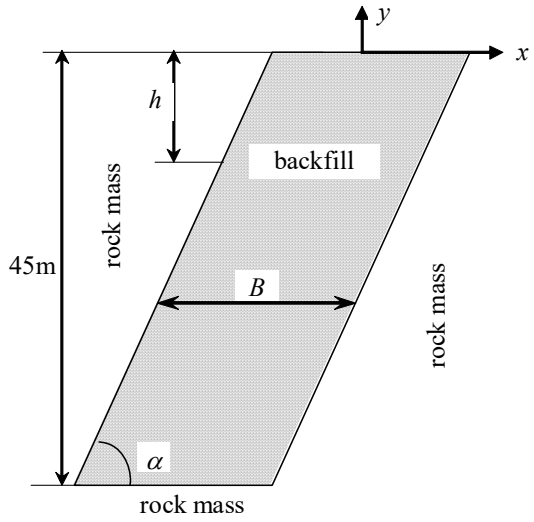

Figure 2. Typical discretization with enlarged view of the backfilled stop

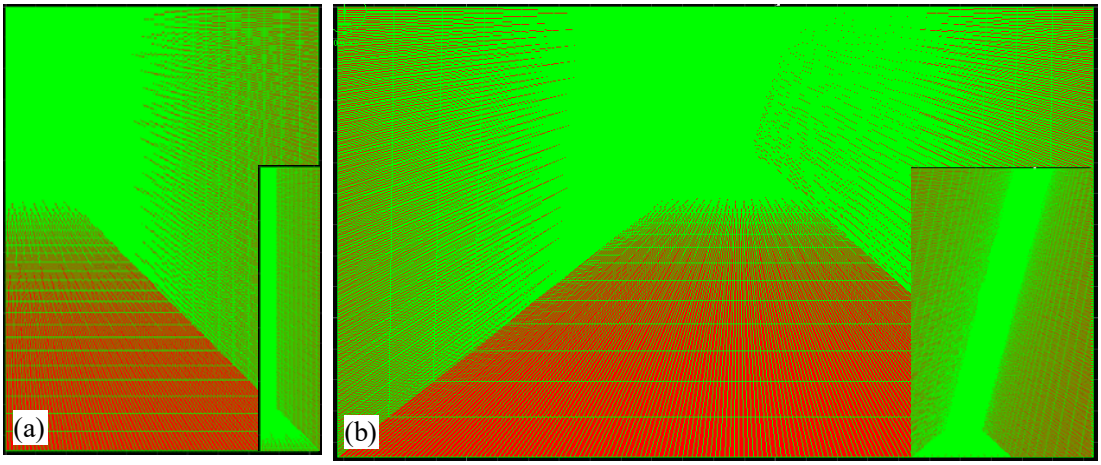

3.1 Asymmetric stress distribution

Typical simulation results are presented in Figure 3 for $\alpha = 80°$, with the following backfill properties: $E = 300$ MPa, $\mu = 0.2$, $\gamma = 18$ kN/m^3, $\phi' = 30°$, $c' = 0$ kPa, $\psi' = 0°$. It is seen that both the horizontal (Fig. 3a) and vertical (Fig. 3b) stresses are usually smaller along the walls than in the central part of the stope, at a given elevation. The stress magnitude increases nonlinearly with depth h at all locations. These indicate the occurrence of arching effects. Contrary to the case of vertical stopes, the stress distribution in inclined stopes is seen to be asymmetric. In the lower parts of the stope (close to the base), the vertical stress ($\sigma_v = \sigma_{yy}$) along the hanging wall becomes smaller than along the foot wall (Fig. 3b). However, the horizontal stress (Fig. 3a) in these lower parts is higher along the hanging wall

than along the foot wall. The normal pressure exerted on the walls, which is dominated here by the horizontal stress component ($\sigma_h = \sigma_{xx}$), is also larger along the hanging wall than along the foot wall. The angle between the minor principal stress (σ_3) and the horizontal axis (Fig. 3c) indicates that the major principal stress (σ_1) makes an angle of about 20° from both the hanging wall and foot wall (which are both at 10° from the vertical in this example). Such principal stress rotation is typical of the arching process (Krynine 1945; Handy 1985, 2004; Li et al. 2003, 2005a).

Table 1. Numerical simulations for stress analyses with stope and backfill properties (γ = 18 kN/m^3); "var" indicates varying values

Figures	α (°)	B (m)	E (MPa)	μ	ϕ' (°)	c' (kPa)	ψ' (°)	layers
3	80	6	300	0.2	30	0	0	4
4	var	6	300	0.2	30	0	0	4
5	75	var	300	0.2	30	0	0	4
6	75	6	var	0.2	30	0	0	4
7	75	6	300	var	30	0	0	4
8	75	6	300	0.2	var	0	0	4
9	75	6	300	0.2	30	var	0	4
10	75	6	300	0.2	30	0	var	4
11	90	6	300	0.2	30	0	0	1
12	90	6	300	0.2	30	0	0	var
13	60	6	300	0.2	30	0	0	var
14	75	6	300	0.2	30	1000	0	4
15	75	6	300	0.2	30	1000	0	4
16	75	6	300	0.2	30	1000	0	var
17	var	6	300	0.2	30	0	0	4
18	75	var	300	0.2	30	0	0	4
19	75	6	300	var	30	0	0	4
20	75	6	300	0.2	30	0	var	4
21	75	6	300	0.2	30	var	0	4

Figure 3. Numerical modelling results for the horizontal (a) and vertical (b) stress distribution and distribution of the minor principal stress angle with respect to the horizontal axis (x) (c) for $\alpha = 80°$; backfill properties: E = 300 MPa, $\mu = 0.2$, $\gamma = 18 kN/m^3$, $\phi' = 30°$, $c' = 0$ kPa, $\psi' = 0°$.

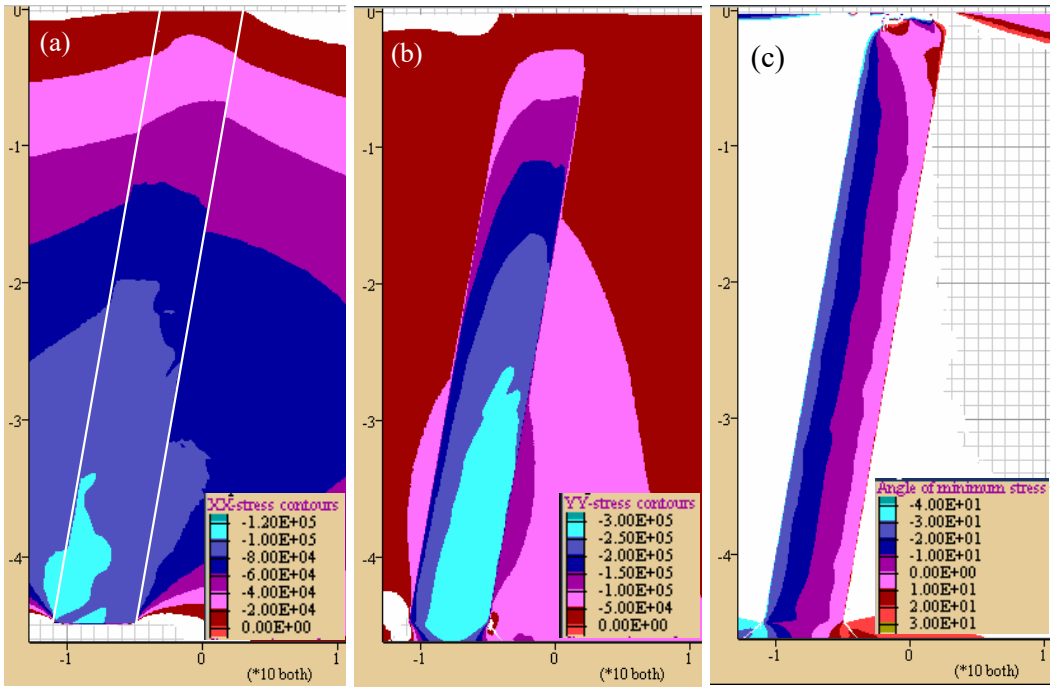

3.2. Effect of the stope geometry

3.2.1 Stope inclination α

Figure 4 shows the variation of stresses across the width at $H/2$ and along the hanging wall, foot wall, and central line when the inclination angle α varies from 90° (vertical) to 60°. The stress distribution over the width indicates that the horizontal stress (Fig. 4a) is not sensitive to the stope inclination. In this case, a uniform σ_{xx} distribution can be considered as an acceptable approximation, as is commonly done in analytical solutions developed for vertical stopes (Aubertin et al. 2003; Li et al. 2005a). For the vertical stress σ_{yy} (Fig. 4a), the distribution is not uniform; this was also observed for the case of a vertical stope (Li et al. 2003). When the walls become more inclined, the stress decreases significantly within the backfill close to the hanging wall. Near the foot wall, the vertical stress increases when the inclination angle varies from 90° to 70°, and then tends to decrease for a more inclined stope (at 60°).

The results also show that the horizontal stress magnitude on the hanging wall can be higher than that on the footwall for α varying between 70° and 80° approximately.

Figure 4. Stress variation for various inclination angles α: (a) at mid-height of the stope; (b) along the central line; (c) along the hanging wall; (d) along the foot wall; other backfill properties are given in Table 1; σ_{xx}: horizontal stress; σ_{yy}: vertical stress.

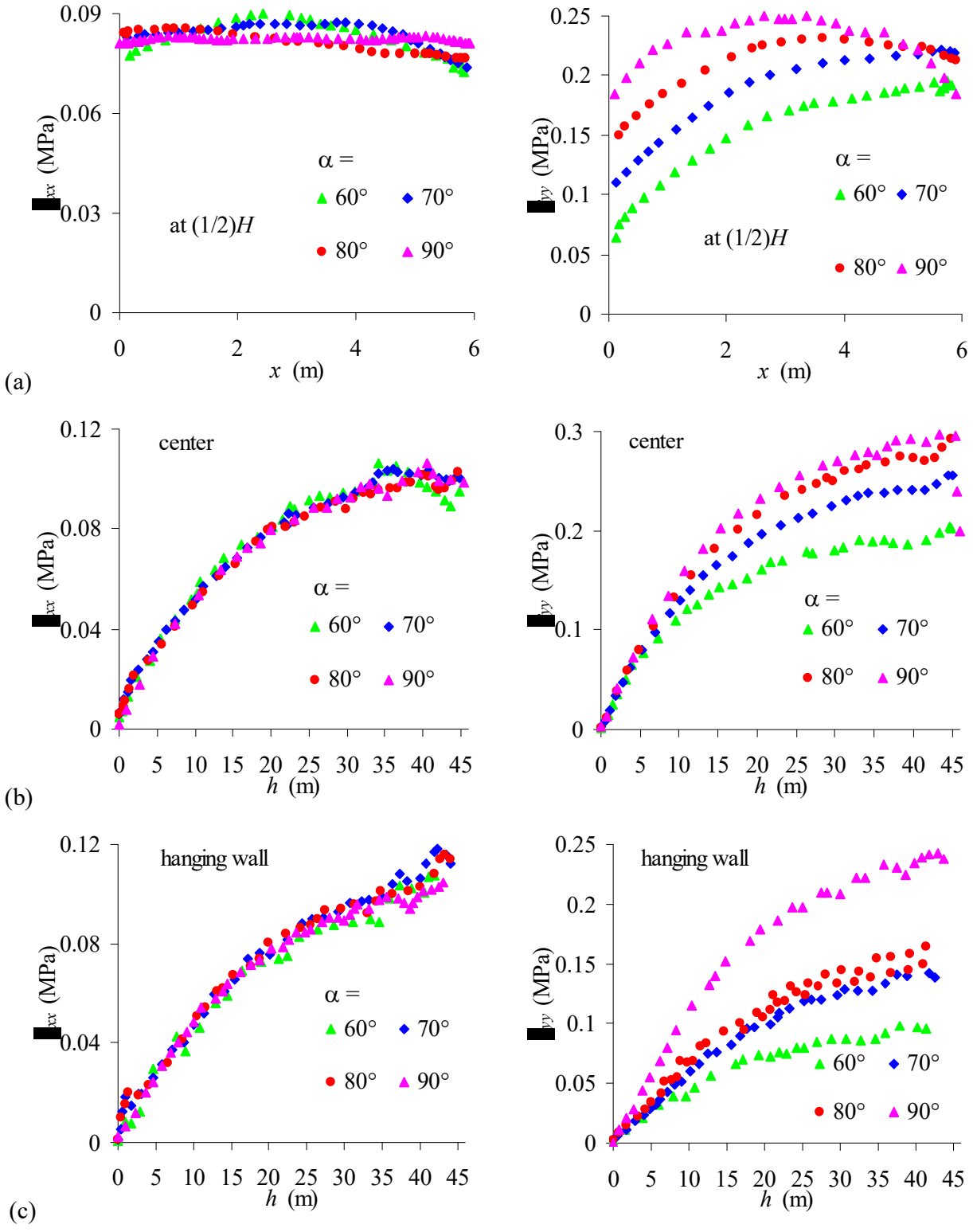

Figure 4(continue).

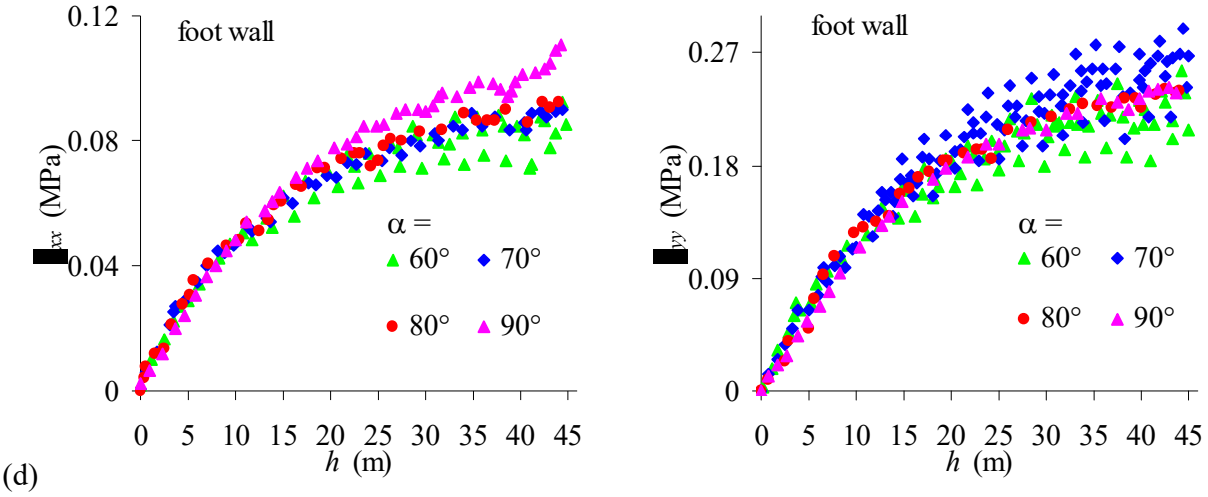

(d)

As for the stress distribution with depth, it is noted that the horizontal stress σ_{xx} is almost insensitive to the change of inclination along the central line (Fig. 4b) and hanging wall (Fig. 4c). However, there is a clear influence of angle α on the stress distribution along the foot wall, especially at greater depth (Fig. 4d). In general, the horizontal stress σ_{xx} tends to decrease when the stope becomes more inclined, but this tendency is not always followed as can be seen when α varies from 90° to 70° along the hanging wall. A reversal of the main tendency is also observed for the vertical stress σ_{yy} along the foot wall, where it is almost unchanged when α varies from 90° to 80°, increases for α = 70°, and then decreases for α = 60°. Along the central line and hanging wall, the vertical stress σ_{yy} decreases when the stope becomes more inclined (i.e. smaller α).

The results shown here (and others not presented) also indicate that stress transfer to the hanging wall may disappear when the stope angle α becomes close to (or less than) the angle of the major principal stress.

The results shown in Fig. 4 suggest that the vertical and horizontal stresses along the central line could be estimated using the solution developed for vertical stopes by Aubertin et al. (2003; see also Li et al. 2003, 2005a), for α ≥ 80°. In this case, the magnitude of the horizontal stress σ_{xx} along the hanging wall and of the vertical stress σ_{yy} along the foot wall is also close to those of the vertical stopes. However, a stope inclination of 80° (or less) induces a significant difference when compared to the vertical stope situation for the horizontal stress along the foot wall and the vertical stress along the hanging wall. Hence, the solution developed for vertical openings would not be applicable to these cases.

3.2.2 Effect of stope width B

The influence of the stope width on the stress distribution has been previously assessed using analytical solutions (e.g., Li et al. 2005a), but there have been few numerical calculations to evaluate this aspect, especially for inclined stopes. Figure 5 shows the stress distribution obtained (with multi-step filling) for the case $\alpha = 75°$ when the stope width B is 3 m and 6 m. As expected, the results show that a decrease of the stope width increases the arching effect, significantly reducing the stress magnitudes in the stope. This observation corresponds well to the predictions made with analytical solutions developed for vertical stopes (Aubertin et al. 2003; Li et al. 2005a).

Figure 5. Stress variation for two stope widths B: (a) at mid-height of the stope; (b) along the central line; (c) along the hanging wall; (d) along the foot wall; other backfill properties are given in Table 1 ($\alpha = 75°$).

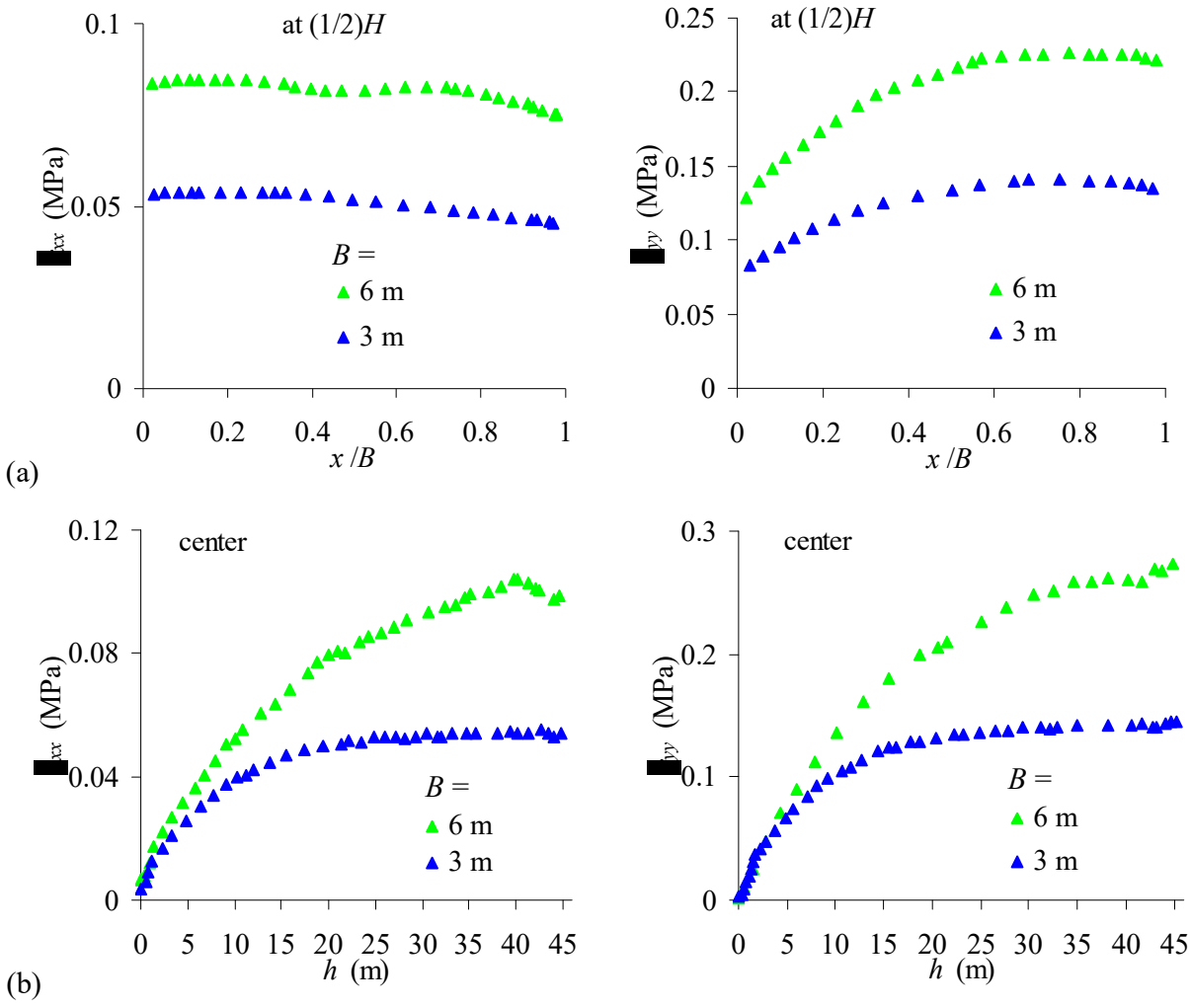

Figure 5 (continue).

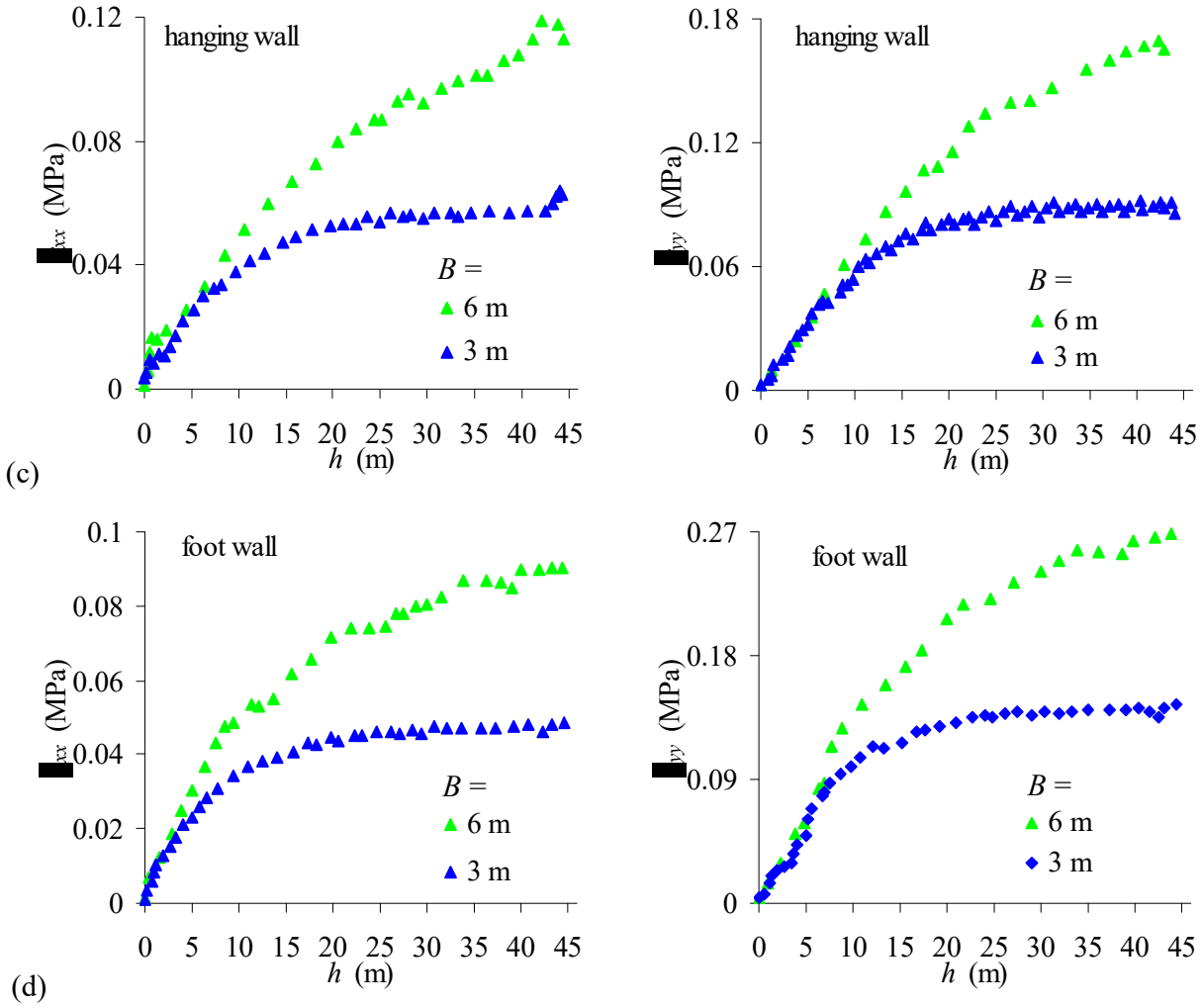

3.3 Effect of backfill properties

3.3.1 Backfill stiffness E

Figure 6 shows the stress distribution (with the multi-step filling sequence) obtained for the case α = 75° when the modulus E is increased from 30 MPa to 3 GPa. One sees that the stress state remains almost unchanged as long as the modulus E is below about 300 MPa. However, when the stiffness is increased to 3 GPa, the stress distribution is modified and it becomes somewhat irregular (oscillatory) in the deeper part of the stope. The modifications indicate a change in the mechanical behavior of the backfill when its stiffness is high. In this latter case, the filling sequence affects the stress distribution.

Figure 6. Stress variation for different backfill moduli E: (a) at mid-height of the stope; (b) along the central line; (c) along the hanging wall; (d) along the foot wall; other backfill properties are given in Table 1 ($\alpha = 75°$).

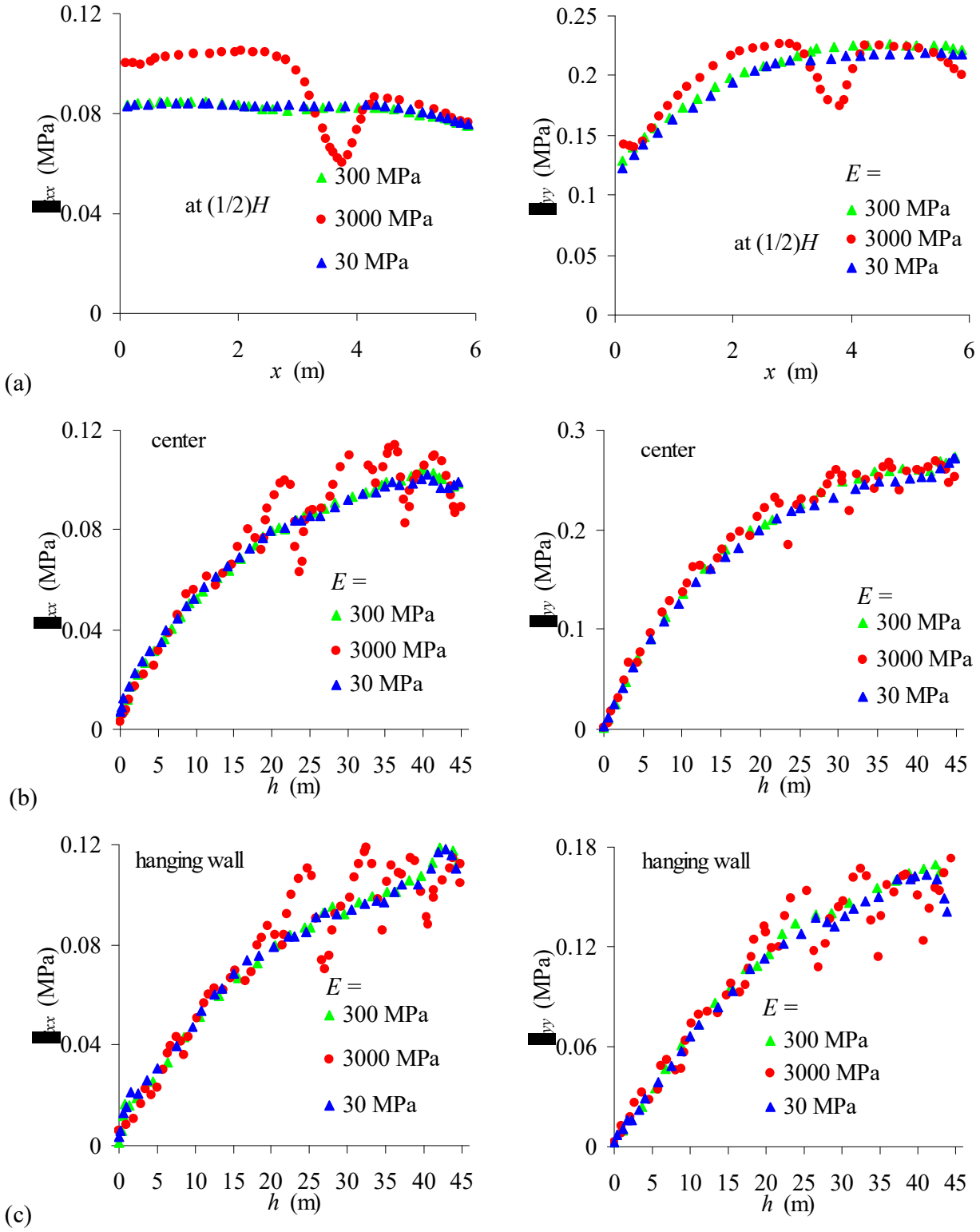

Figure 6 (continue).

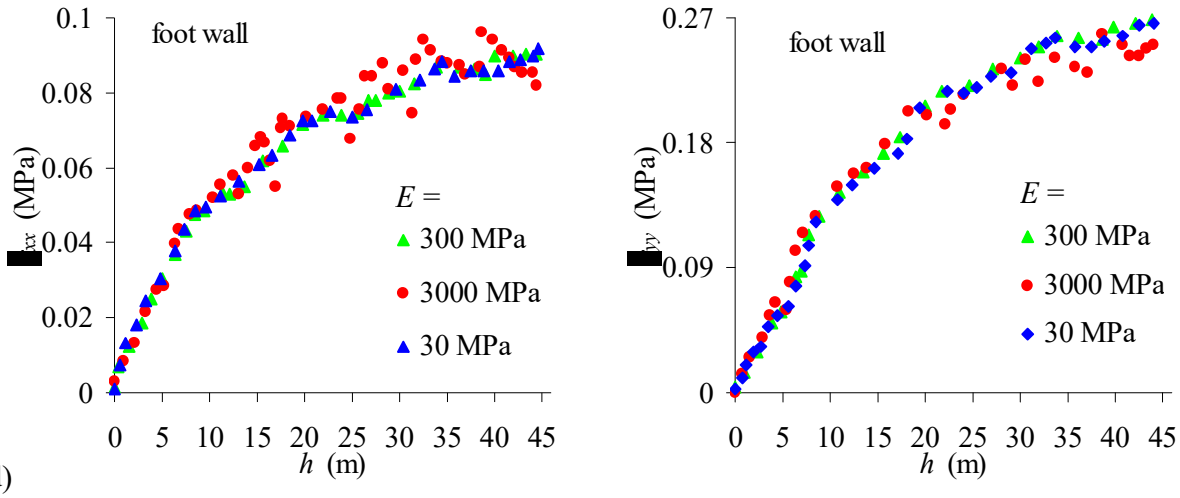

3.3.2 Poisson's ratio μ

The stress distribution obtained for various μ values is shown in Figure 7. It is seen that the vertical stress σ_{yy} in the stope is very sensitive to variations of the Poisson's ratio, while the horizontal stress σ_{xx} is less affected. In general, an increase of the Poisson's ratio tends to increase the horizontal stress σ_{xx} and to reduce the vertical stress σ_{yy} magnitude. Increasing the value of μ also affects the regularity of the stress distribution (see Figs. 7b and 7c); a large μ value may increase the effect of the filling sequence.

3.3.3 Friction angle ϕ'

Figure 8 presents the stress variations as a function of the backfill friction angle ϕ'. At first glance, it appears that both stresses (σ_{xx}, σ_{yy}) decrease in the stope with an increase of the friction angle values. However, when the friction angle is greater than about 20°, the vertical stress becomes almost insensitive to any further increase of ϕ' (see Fig. 8). This particular response has also been predicted by calculations made with analytical solutions (Aubertin et al. 2003; Li et al. 2005a).

Figure 7. Stress variation for different backfill Poisson's ratios μ: (a) at mid-height of the stope; (b) along the central line; (c) along the hanging wall; (d) along the foot wall; other backfill properties are given in Table 1 (α = 75°).

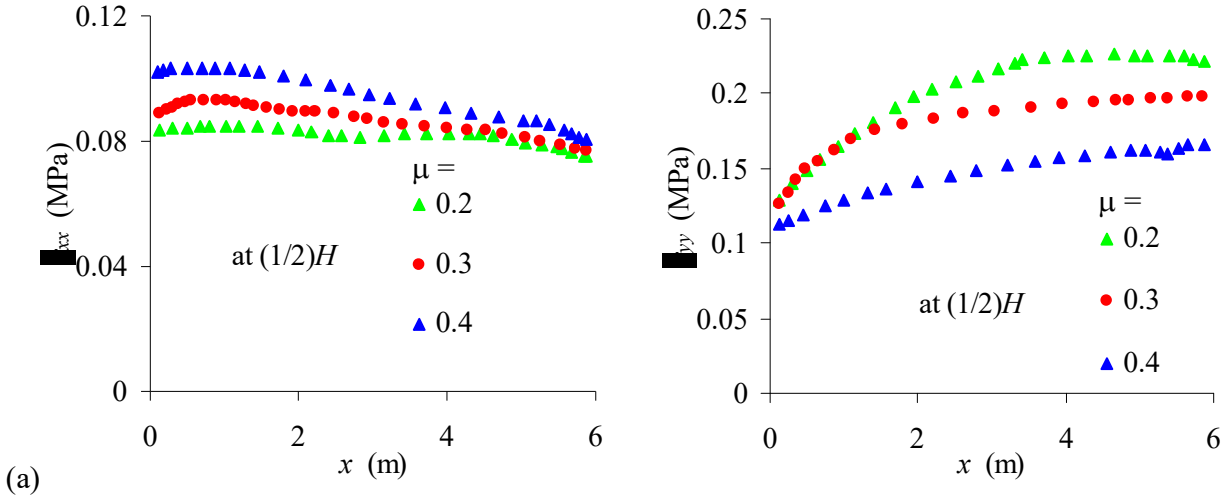

(a)

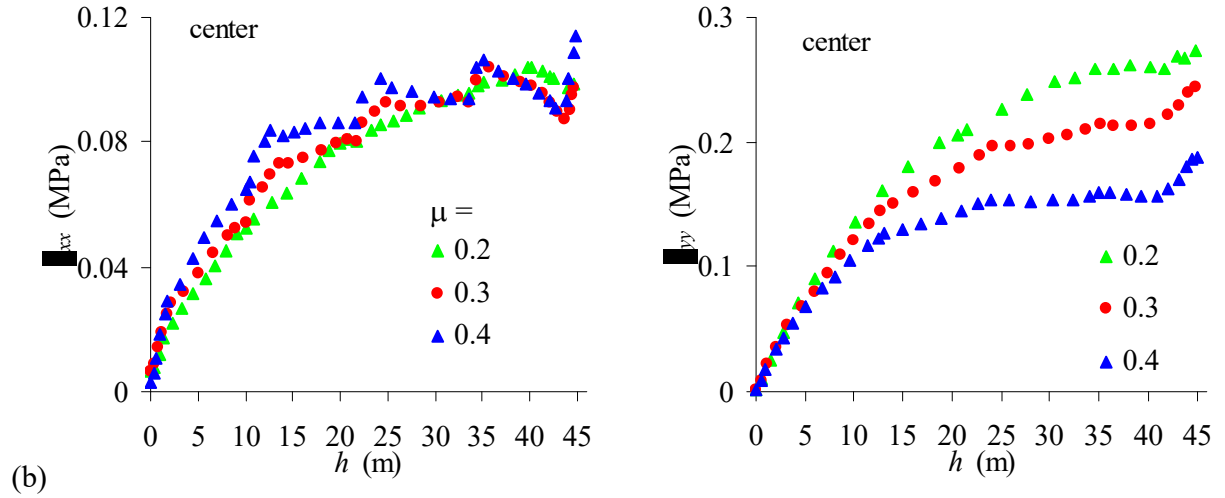

(b)

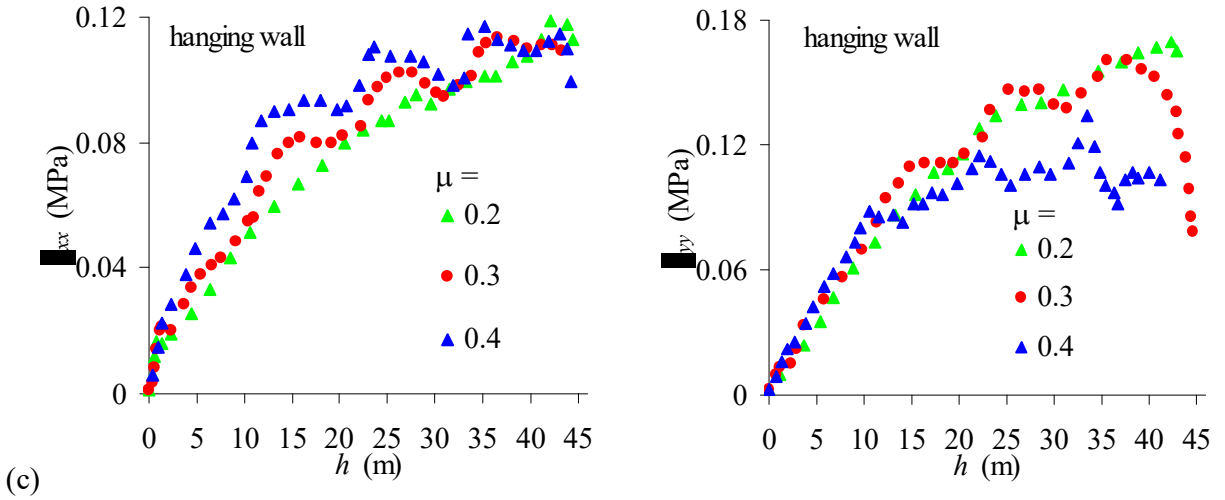

(c)

Figure 7 (continue).

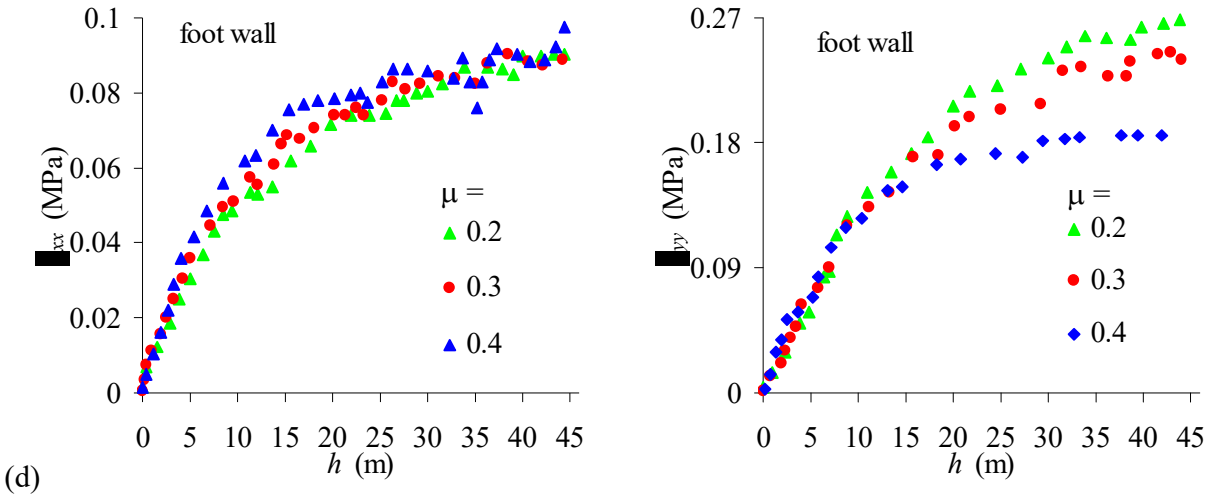

(d)

3.3.4 Cohesion of backfill c'

Li et al. (2007) have shown (using a pseudo-static approach with a single step filling sequence) that the stress distribution in stopes can be quite sensitive to the magnitude of the backfill cohesion *c*'. Results obtained with multi-step filling are shown in Figure 9. It can be seen that the influence of cohesion appears limited to values between 10 kPa and 50 kPa. When the fill cohesion is low (<10 kPa) or when it is relatively large (>59 kPa), both the horizontal and vertical stress distributions are quite regular along the central line of the stope and stope walls. When 10 kPa ≤ *c*' ≤ 50 kPa, Figure 9 shows (among other features) that the stresses are less uniform, becoming oscillatory (or wavy). The position of the troughs corresponds to the interfaces between the layers. This is indicative of change in the mechanical behavior of the backfill, from a particulate material response to that of a solid (consolidated) material (with each layer behaving somewhat like a beam). The horizontal stress at the center of the stope then reaches a local maximum at the top of each layer and a minimum at their base (Fig. 9b). The vertical and horizontal stresses along the two walls show a local maximum near (but above) the mid-height of each layer (Figs. 9c and 9d).

3.3.5 Dilatation angle ψ'

Figure 10 shows that dilatation of the backfill may also affect the stress distribution in stopes. Across the width, an increase of the dilatation angle ψ' makes the horizontal stress distribution less uniform, while it appears to have the reverse effect on the vertical stress distribution. In general, a higher

dilatation angle reduces the vertical stress. Again, the influence of ψ' is related to the layering sequence. The degree of oscillations in the stress distribution waviness tends to increase with the dilatation angle ψ'. Both the vertical and horizontal stresses along the two walls show a local maximum value near the mid-height of each layer (Fig. 10b), also is the horizontal stress along the central line of the stope (Fig. 10a for ψ' > 0°).

Figure 8. Stress variation for different backfill friction angles ϕ': (a) at mid-height of the stope; (b) along the central line; (c) along the hanging wall; (d) along the foot wall; other backfill properties are given in Table 1 (α = 75°).

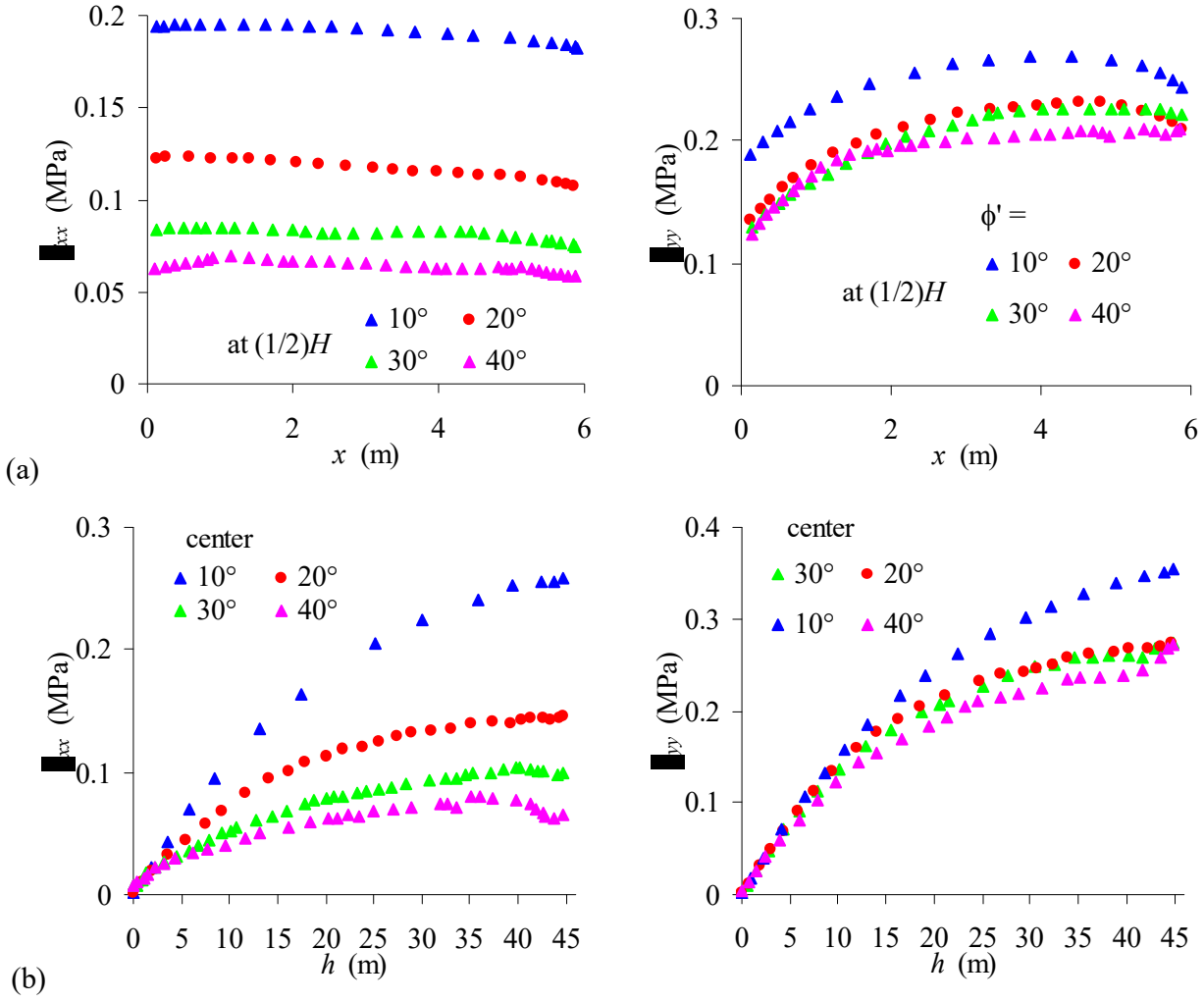

Figure 8 (continue).

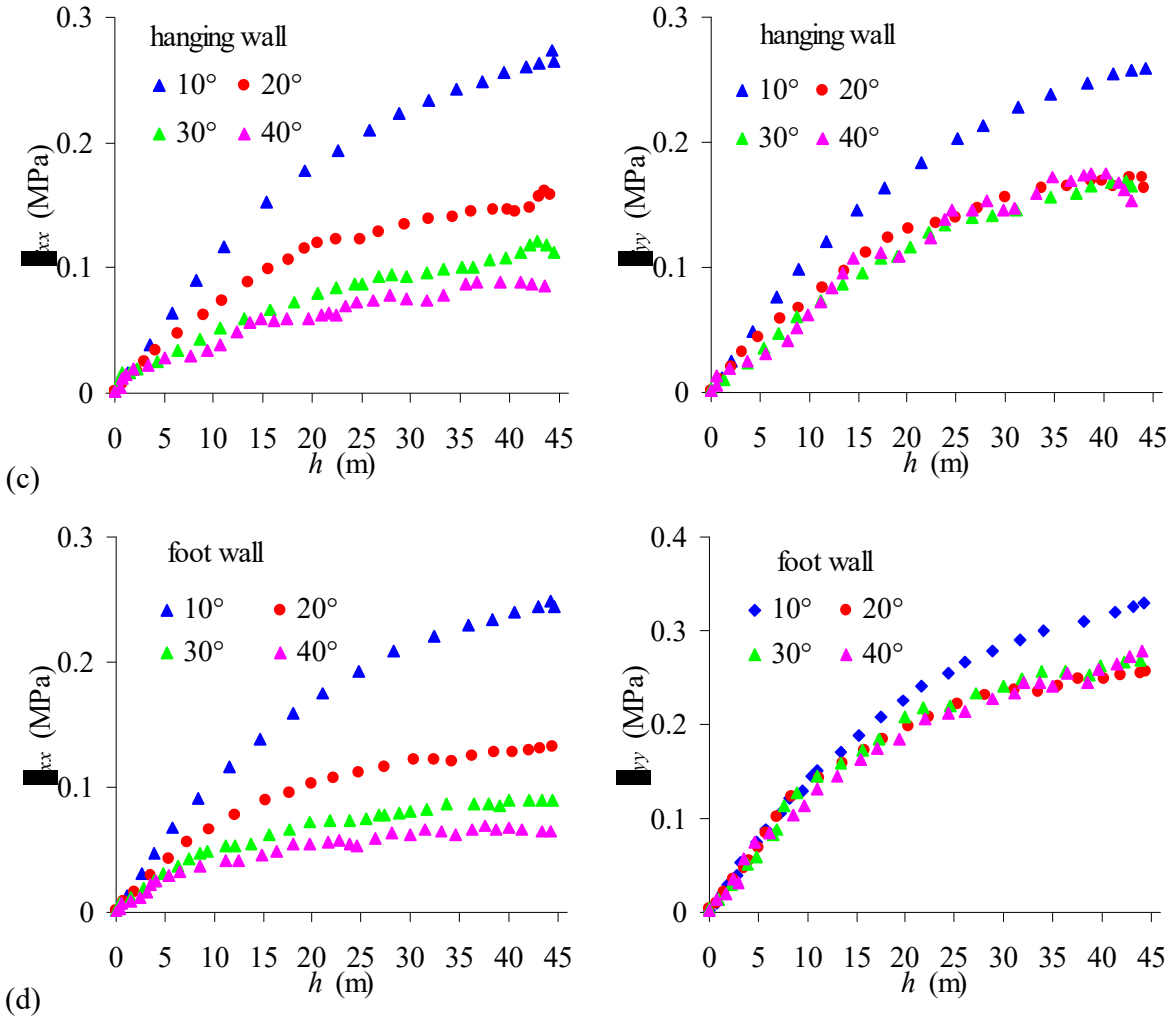

4. RESULTS ANALYSIS AND DISCUSSION

4.1 Influence of meshing

As with any numerical discretization scheme, a preliminary modeling step with FLAC should serve to determine a valid mesh configuration. It is well known that a mesh size that is too coarse may lead to erroneous results, while an overly fine mesh may needlessly increase the CPU time (and may create convergence problems in some cases). Thus, the discretization should be optimized so the mesh is as coarse as possible without compromising the simulation results. This assessment was performed early in this investigation to obtain a reliable mesh size. To illustrate the potential influence of meshing, the authors show results obtained herein for a vertical stope (α = 90°) with the following backfill properties: E = 300 MPa, μ = 0.2, γ = 18 kN/m^3, ϕ' = 30°, c' = 0 kPa, and ψ' = 0° (non associated flow

rule). The stresses calculated with different meshes at $H/2$ and along the vertical central line are shown in Figure 11 (meshing 1: 60×180; meshing 2: 120×360; meshing 3: 240×720; meshing 4: 360×720). These results indicate that an optimum discretization would correspond to meshing 3, based on the stress state in the rock mass (Fig. 11b). However, results shown in Figure 11 also indicate that the stress state at the fill-wall interface (just before the abrupt stress change) obtained with the coarser mesh (meshing 1) gives results almost identical to those obtained with the finest mesh (meshing 4). This example serves to explain how the mesh sizes have been chosen for this study (i.e. 60×180 elements for vertical stopes and 120×180 elements for inclined stopes – see Fig. 2b).

Figure 9. Stress variation for different backfill cohesion c': (a) at mid-height of the stope; (b) along the central line; (c) along the hanging wall; (d) along the foot wall; other backfill properties are given in Table 1 (for α = 75°).

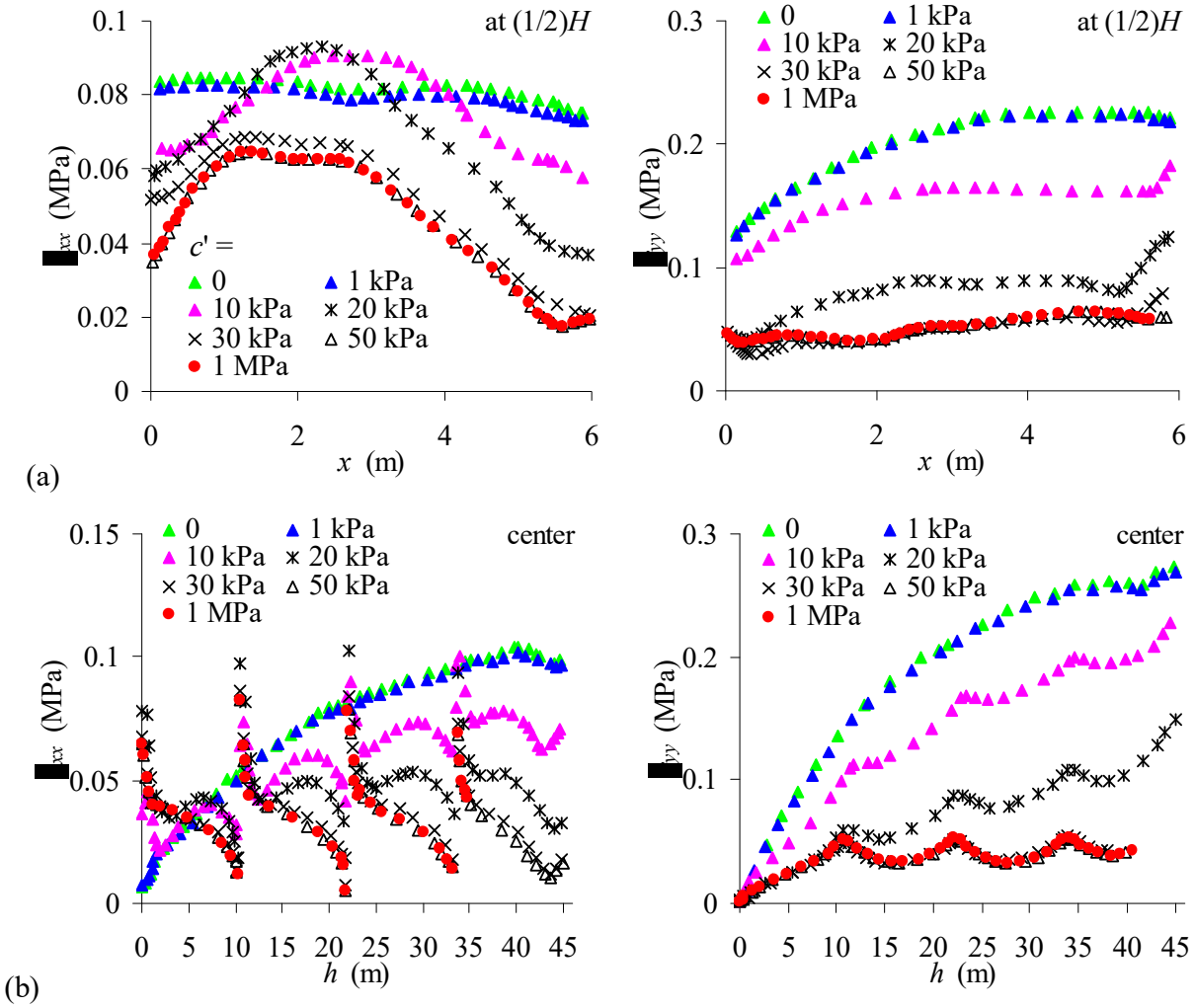

Figure 9 (continue).

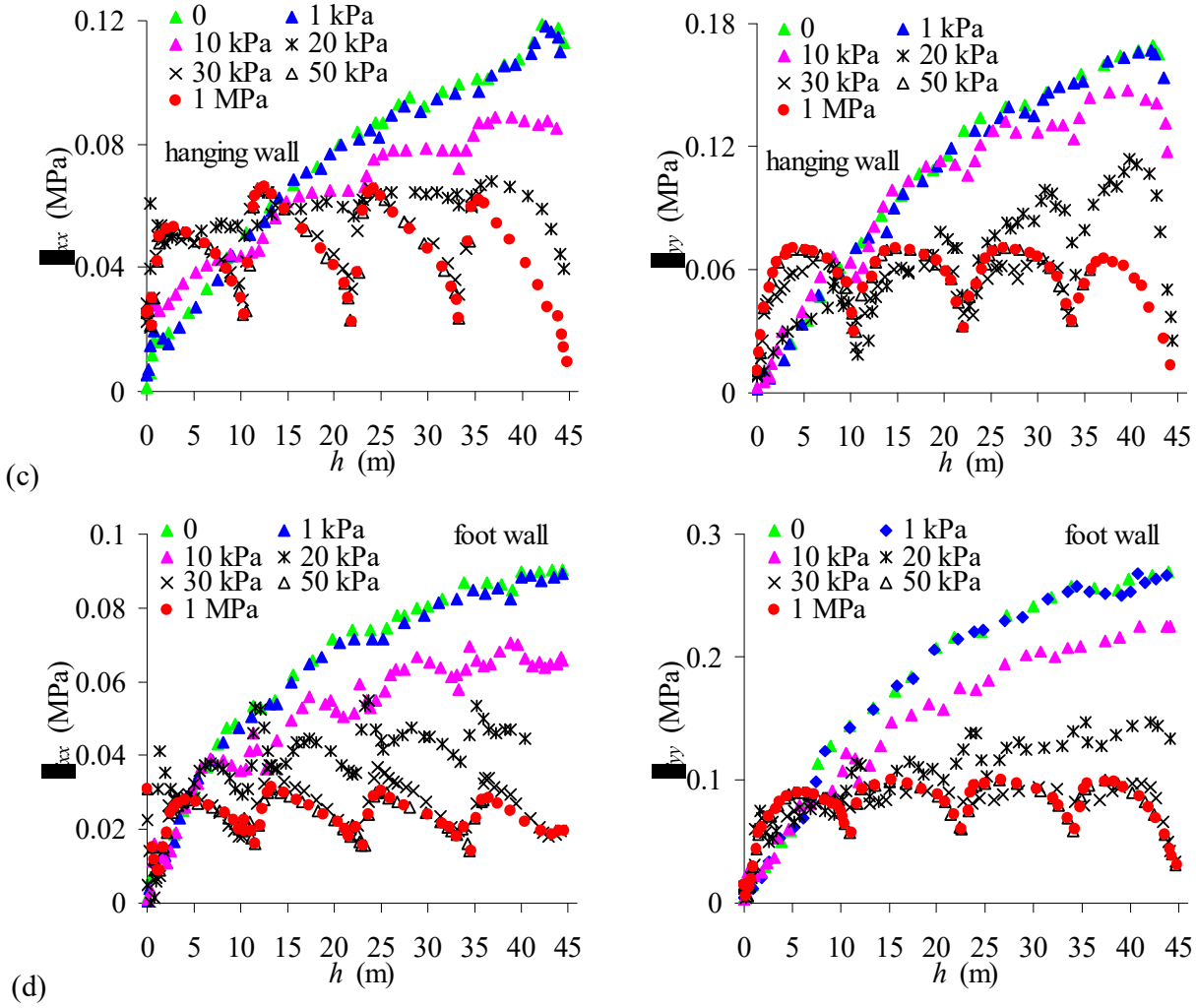

4. 2 Effect of layering (filling) sequence

In FLAC, the dynamic equations of motion are used, even when the model represents a static system (Itasca 2002). In previous studies, the authors initially used a pseudo-dynamic approach (Li et al. 2003) to obtain the stress state; this approach tends to overestimate the stress magnitude in the stopes. More recently, a pseudo-static procedure was used where the backfilled stope was simulated using a one-step filling sequence (Li et al. 2007). Pirapakaran and Sivakugan (2007b) have presented an alternative multi-step simulation procedure to obtain a static solution. Figure 12 shows a comparison between the stress distribution obtained with the pseudo-dynamic and pseudo-static methods (with a single layer) and with a multi-step filling simulation. As can be seen, the stresses obtained with the different approaches are fairly close to each other. The results nonetheless indicate that the pseudo-dynamic and

pseudo-static calculations (with one step) tend to overestimate the stress state when compared to a multi-layer sequence. The results shown in Fig. 12 also show that simulations with four steps (or layers) can be considered as representative of the static (at 10 steps) solution because results do not change significantly when adding more layers (for the case at hand). This is confirmed by results shown in Figure 13 which show that simulations of an inclined stope with four and eight layers are practically equivalent. This justifies the use of 4 layers in the numerical modeling results presented above. Nonetheless, it should be noted that for a dilatant or highly cohesive backfill, the number of filling layers may play an important role due to the particular mechanical response of the backfill (see paragraphs below).

Figure 10. Stress variation for different backfill dilatation angles ψ': (a) at mid-height of the stope; (b) along the central line; (c) along the hanging wall; (d) along the foot wall; other backfill properties are given in Table 1 (for α = 75°).

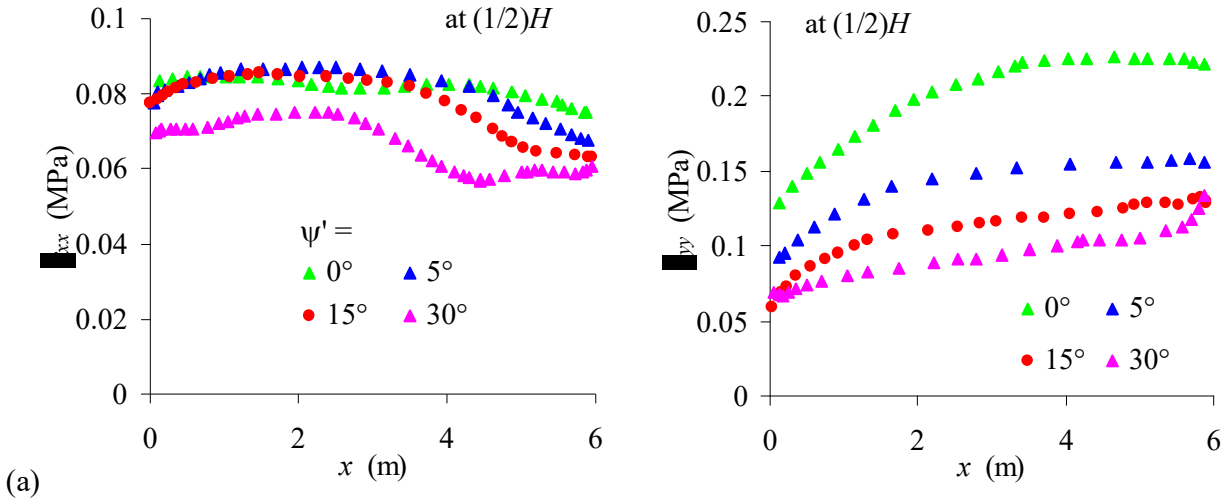

Figure 10 (continue).

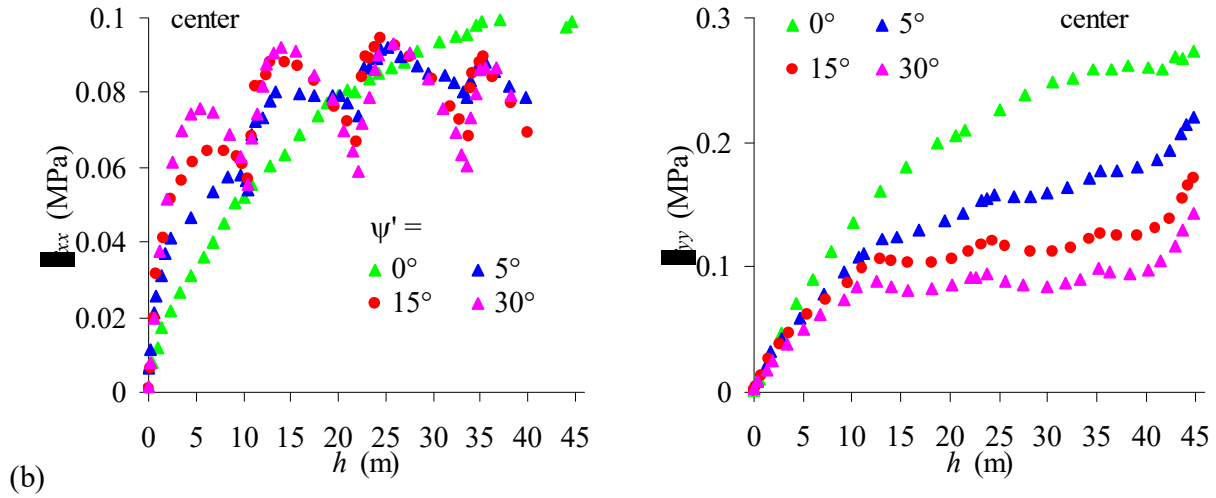

(b)

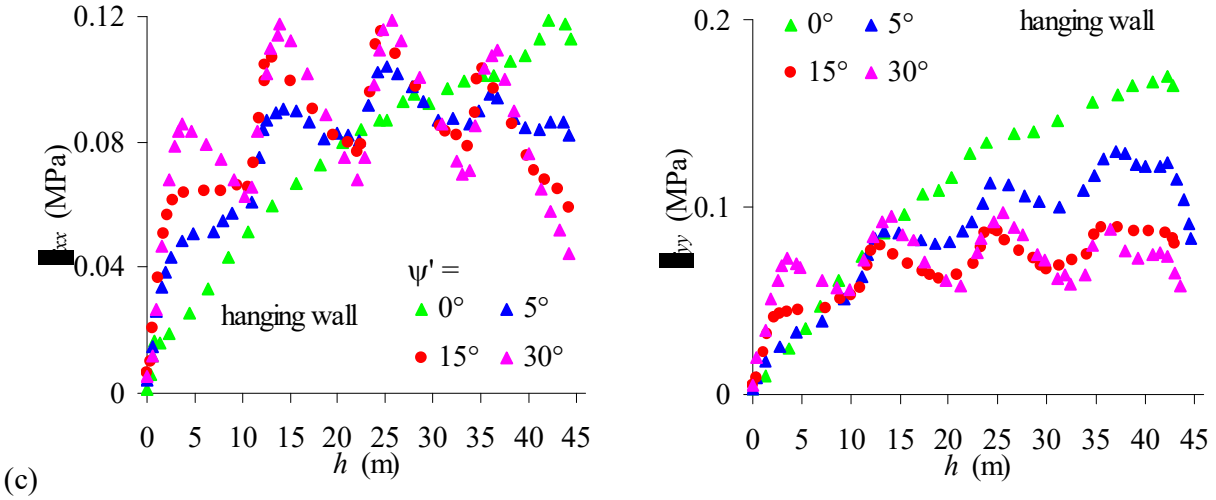

(c)

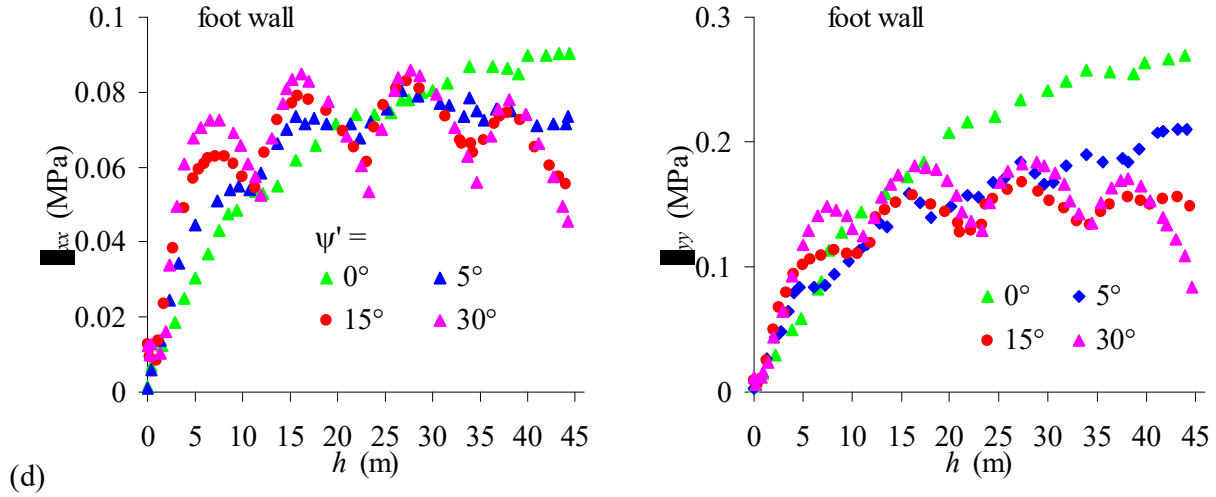

(d)

Figure 11. Stress calculated with different meshes: (a) horizontal stress at $H/2$; (b) vertical stress at $H/2$; (c) a zoom view of (a); (d) horizontal stress along the vertical center-line; (e) vertical stress along the vertical center-line; (f) a zoom view of (d).

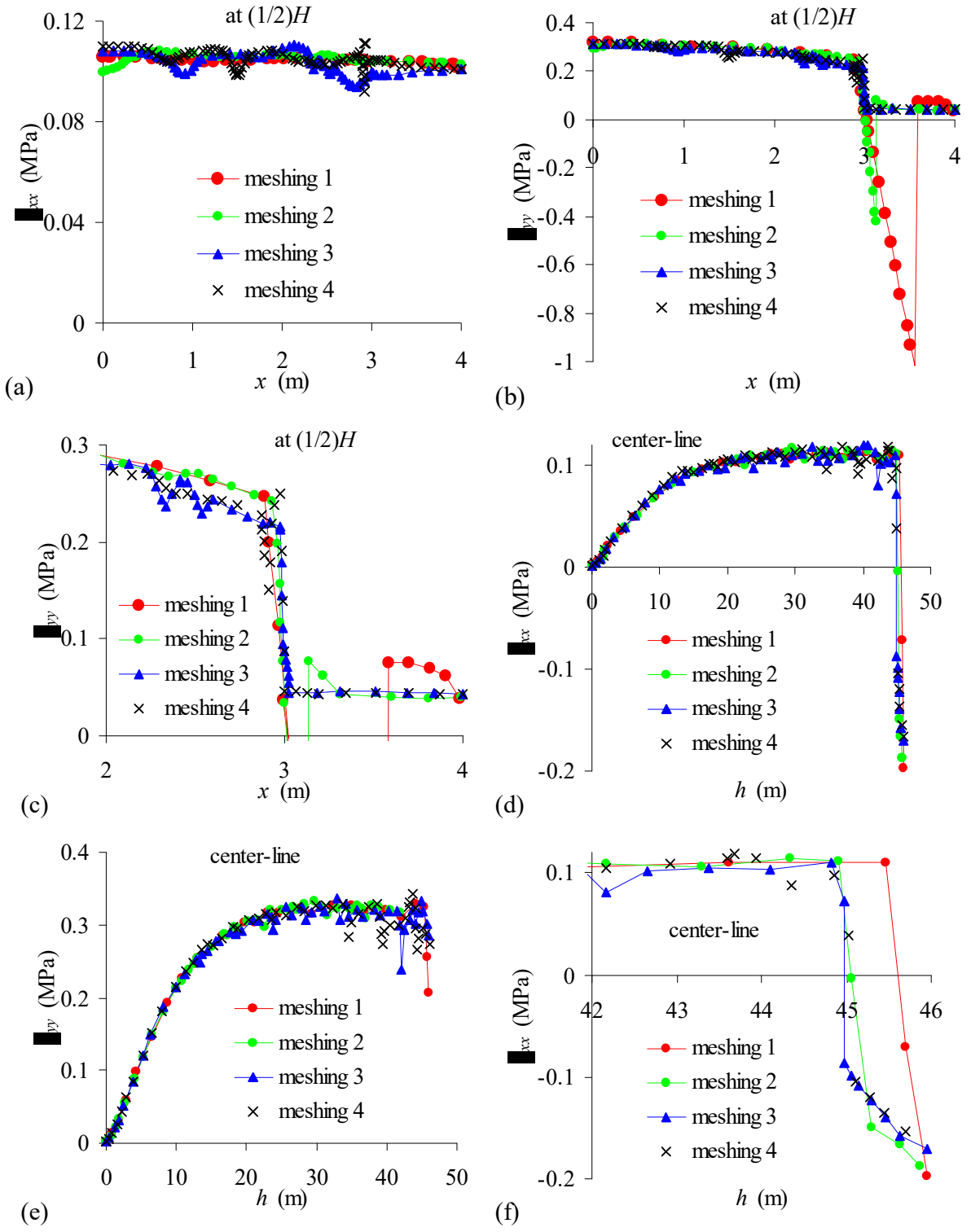

Figure 12. Stress distribution obtained with pseudo-dynamic, pseudo-static and multi-step backfilling simulations: (a) horizontal stress at $H/2$; (b) vertical stress at $H/2$; (c) horizontal stress along the vertical central line; (d) vertical stress along the vertical central line.

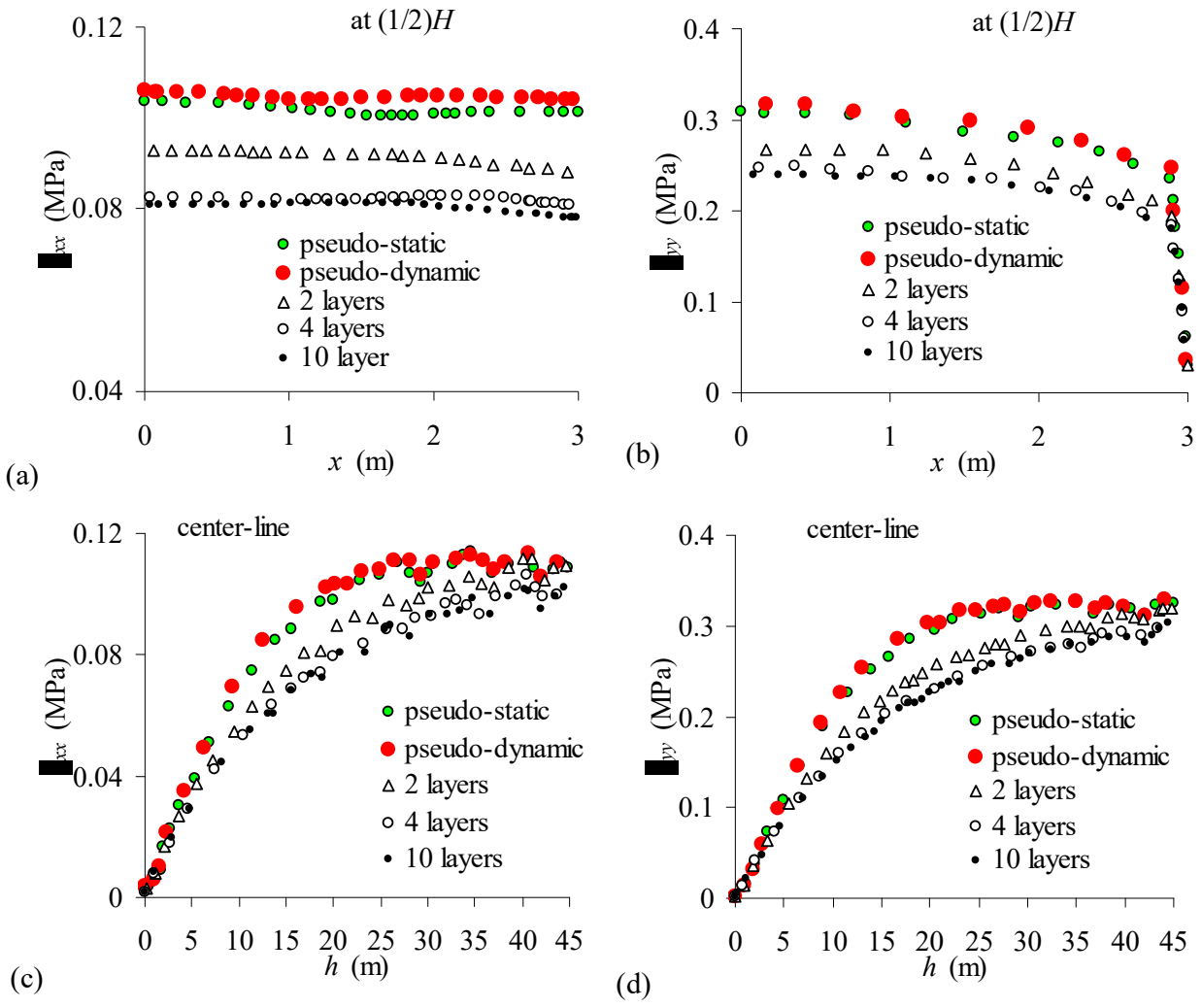

4.3 Multi-layer simulations for cohesive backfill

Results shown above indicate that the stresses in stopes may become oscillatory with depth when the backfill has a relatively high cohesion (or high dilatation angle).

Figure 14 shows the stress distribution obtained from a multi-step filling simulation for c' = 1 MPa (high cohesion). When compared to the case of a cohesionless backfill (Fig. 3), it is seen that the pattern of the stress distribution within the backfill changes markedly. The stresses in a cohesionless fill increase gradually with depth, from the top to the base of the stope (Fig. 3), but the distribution in the case of highly cohesive backfill shows the appearance of four sub-levels (corresponding to the four layers). In each layer, the horizontal stress along the central line of the stope reaches its maximum

value near the top and decreases with depth (instead of increasing) to a local minimum at the base; this was also seen in Fig. 9. This distribution is typical of a beam-like response for each layer.

Figure 13. Stress distribution when backfilling simulated with 4 and 8 steps (each step corresponds to one layer) respectively for α = 60°: (a) at mid-height of the stope; (b) along the central line; (c) along the hanging wall; (d) along the foot wall.

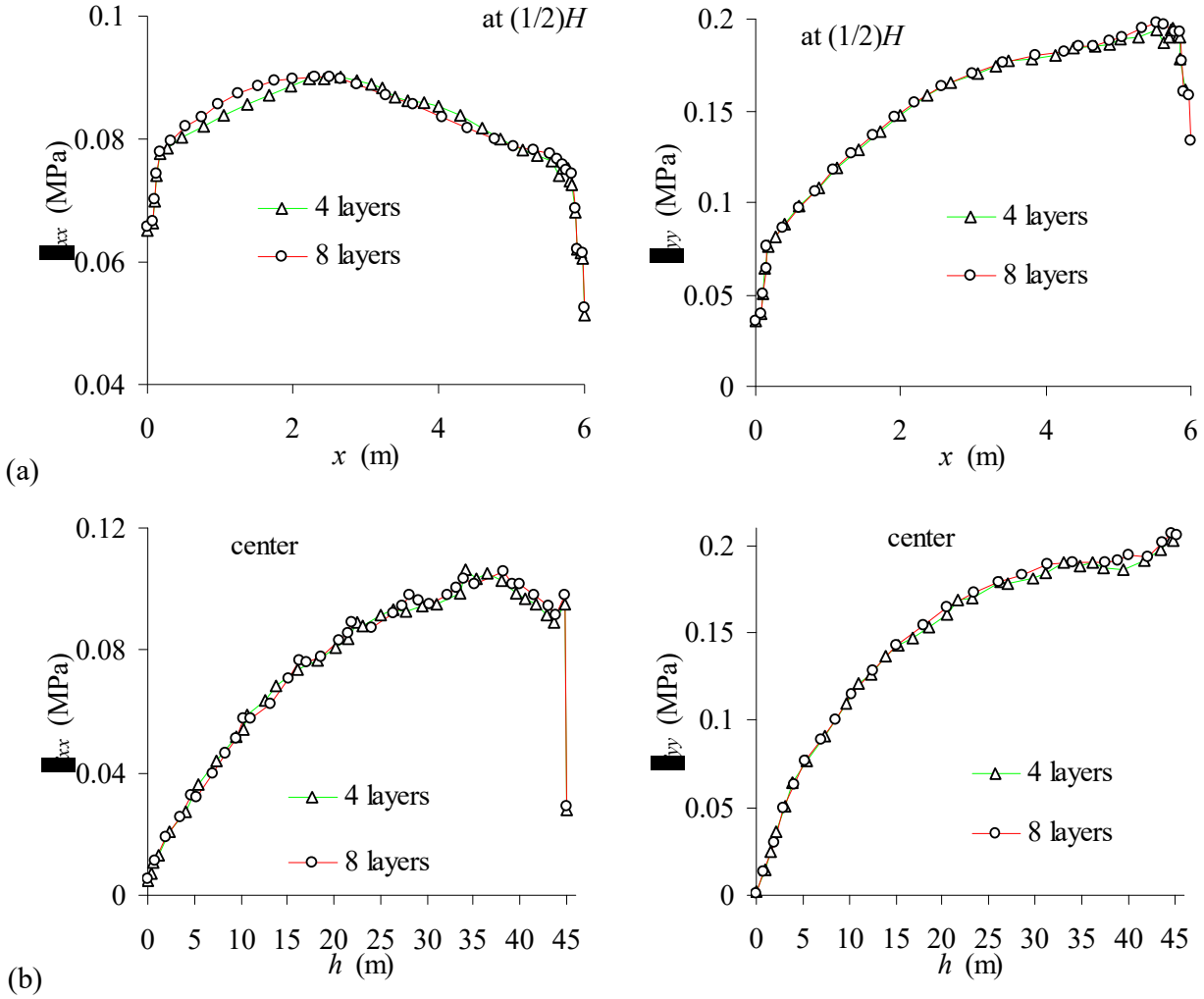

Figure 13 (continue).

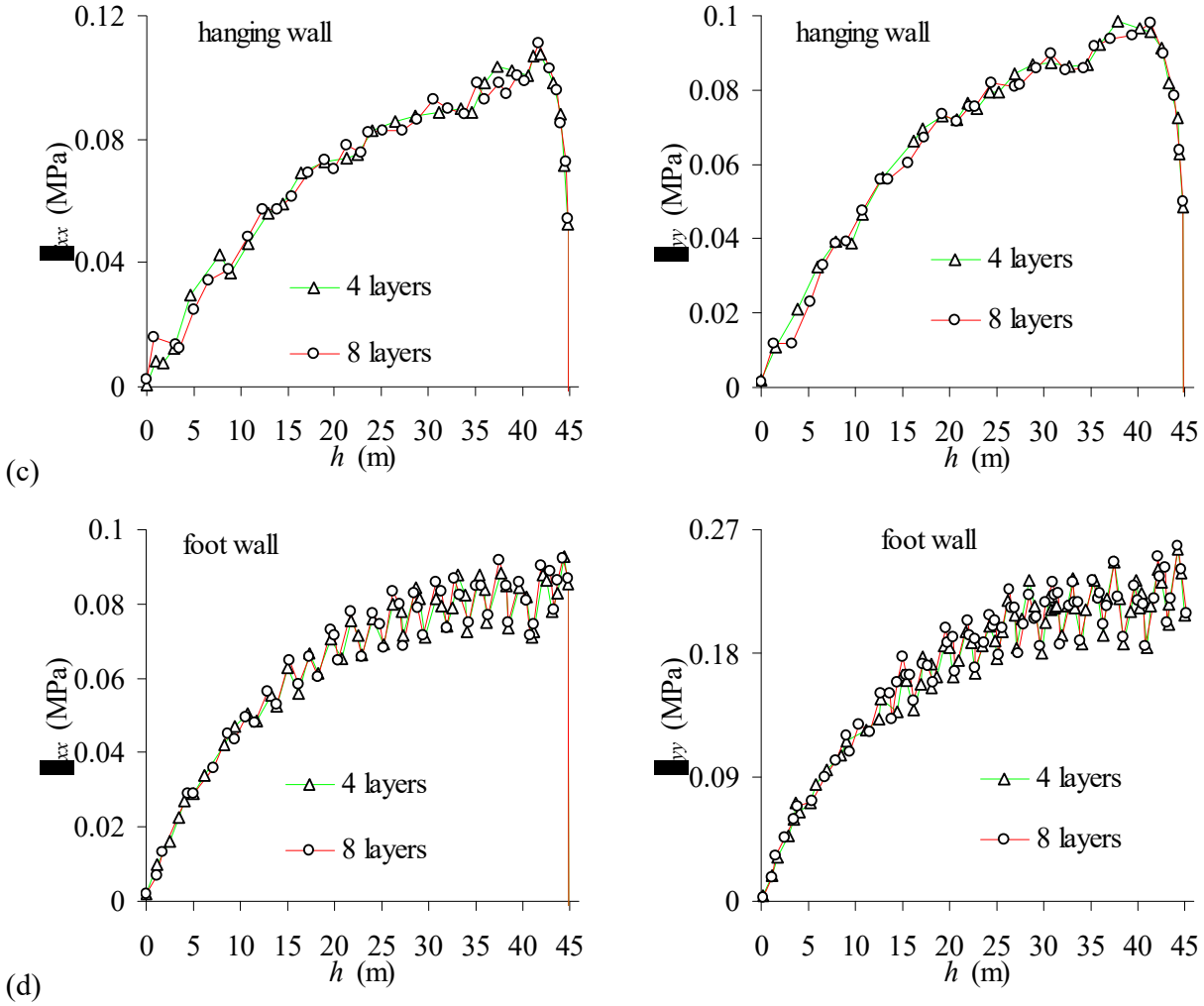

To further assess the nature of the observed stress distribution with depth for highly cohesive backfill, Fig 15 shows the displacement vectors in the stope (for the case of c' = 1 MPa). It can be seen that the displacement magnitude (and orientation) may change abruptly, particularly around interfaces between layers. This figure also shows that the displacement across the width of the stope has the largest downward magnitude in the central part while it becomes minimal close to the walls. This response is very similar to that of a beam subjected to downward bending. The upper portion of each layer is subjected to a compressive stress while the lower part may be subjected to a low compression (or even an extension in some extreme cases). This view helps to explain the stress distributions observed in Figs. 9 and 10.

Figure 16 shows that the stress distribution varies with the number of layers (for the case of c' = 1 MPa), indicating more spread in the stress fluctuations when the number of layers is increased. Thus, for high cohesion backfill, the simulations should be based on the actual filling sequence and layer thicknesses to obtain representative results for the stress distribution in a backfilled stope.

Figure 14. Stress contours showing the development of interfaces between layers.

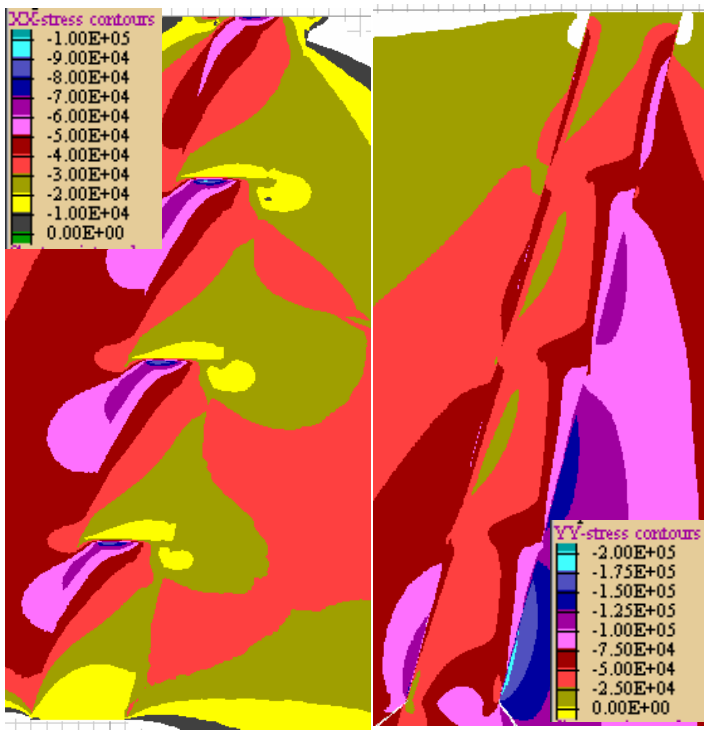

4.4 Stresses along the fill-wall interfaces

Results from the mesh size assessment (Fig. 11) indicate that the vertical stress is subjected to an abrupt change within the backfill close to the wall. The same phenomenon has also been observed for the vertical stress within the backfill close to the floor of the opening. In this report, and in related work (Li and Aubertin 2008a, b), the σ_{xx}, and σ_{yy} magnitudes before the sudden fall are used to represent the stresses along the hanging wall or foot wall. The stress state very close to the interface can be unstable, and may depend on the local mesh size and other modeling parameters. Thus, the stresses presented above should be strictly identified as those near the walls.

Figure 15. Displacement vectors with enlarged views of layer interfaces.

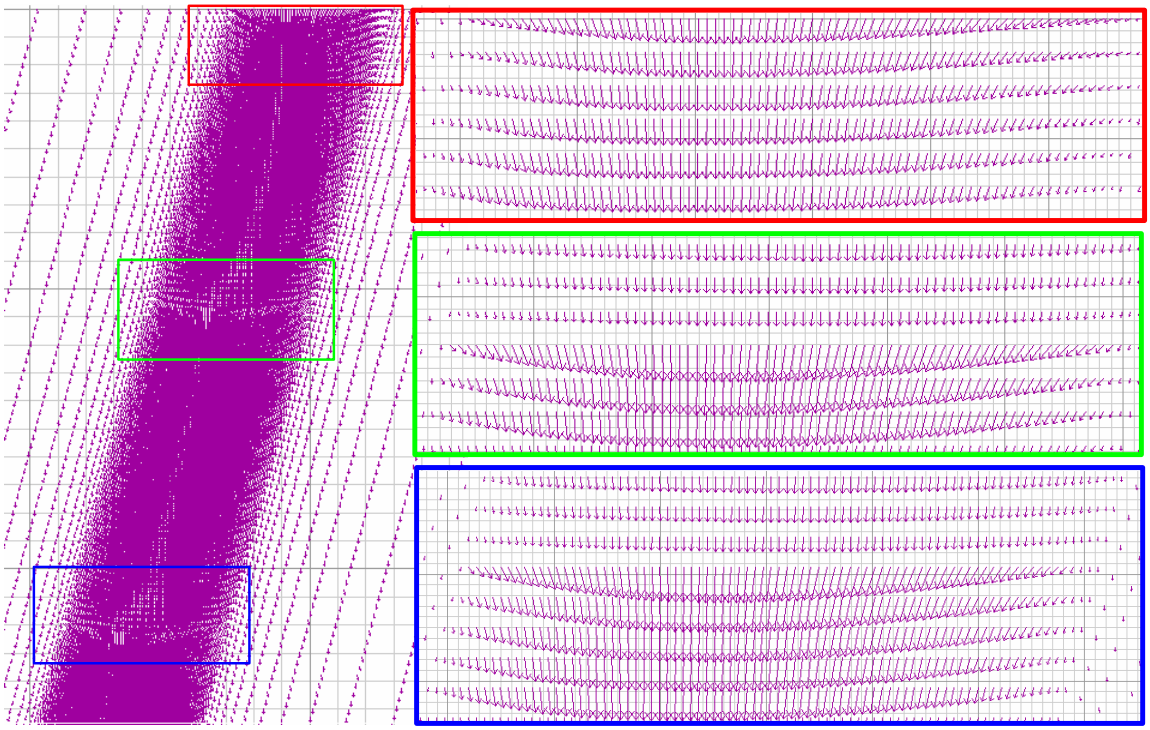

4.5 Assessment of stress distribution

As mentioned above, the authors have also investigated the stress distribution in backfilled stopes with FLAC-2D using a pseudo-dynamic approach (Li et al. 2003) and with a pseudo-static method (Li et al. 2007). Results shown here (with a multi-step sequence) are often quite similar to those previously obtained (for similar situations). There are, however, differences in the stress magnitudes which are mainly due to the different filling sequences. For instance, with the one-layer pseudo-static simulation, the entire backfill is placed in the stope in a single step and this sudden addition of the backfill induces a shock load in the stope. The stress state is then affected by the fill properties which are given a fictitiously high strength, leading to a state of low vertical stress and high horizontal stress. When more realistic properties are subsequently attributed to the backfill, a large part of the lateral support provided by the horizontal and shear stresses along the walls disappears. This leads to another transient loading phase within the backfill. The end results after stress stabilization give magnitudes (with the pseudo-static method used by Li et al. 2007) that are less than those obtained with the pseudo-dynamic method (as used by Li et al. 2003), but somewhat higher than those obtained with the multi-step filling simulation (Fig. 12). The latter is deemed to provide a solution that is closer to a completely static system.

Figure 16. Stress variation along the inclined central line of the stope obtained with different simulation sequences (for α = 75° and c' = 1 MPa); other backfill properties are given in Table 1.

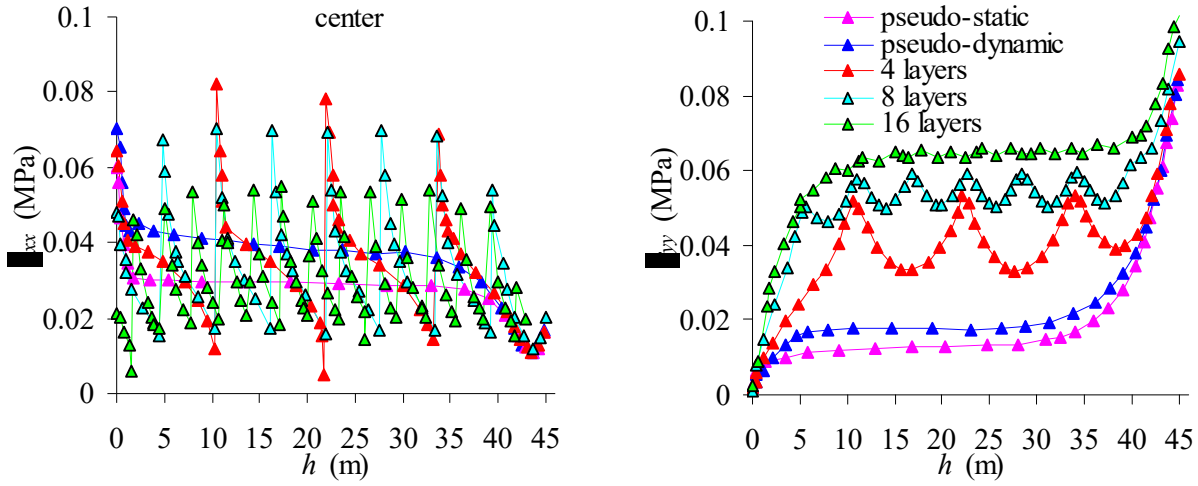

Figure 17. Variation of earth pressure coefficient K (= σ_h'/σ_v') for different stope inclinations α: (a) at mid-height of the stope, (b) along walls; other backfill properties are given in Table 1.

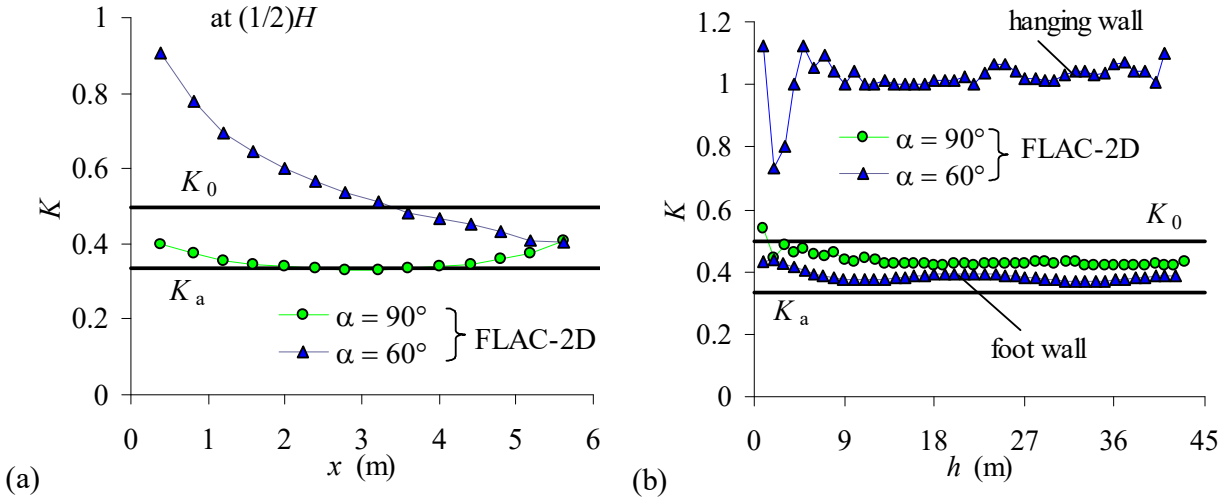

It can be revealing to take into specific result with mode details and compare them to those obtained previously. Fig. 4 shows that the stress magnitude on the hanging wall becomes higher than that on the footwall for α between 70° and 80°; this tendency cannot be anticipated from classical limit equilibrium analyses. These results are also different than those obtained with the pseudo-static method (Li et al. 2007), where stresses appear to be much more sensitive to an angle variation.

Figure 18. Variation of earth pressure coefficient K for two stope widths B: (a) at mid-height of the stope, (b) along hanging wall, (c) along foot wall; other backfill properties are given in Table 1 (for $\alpha = 75°$).

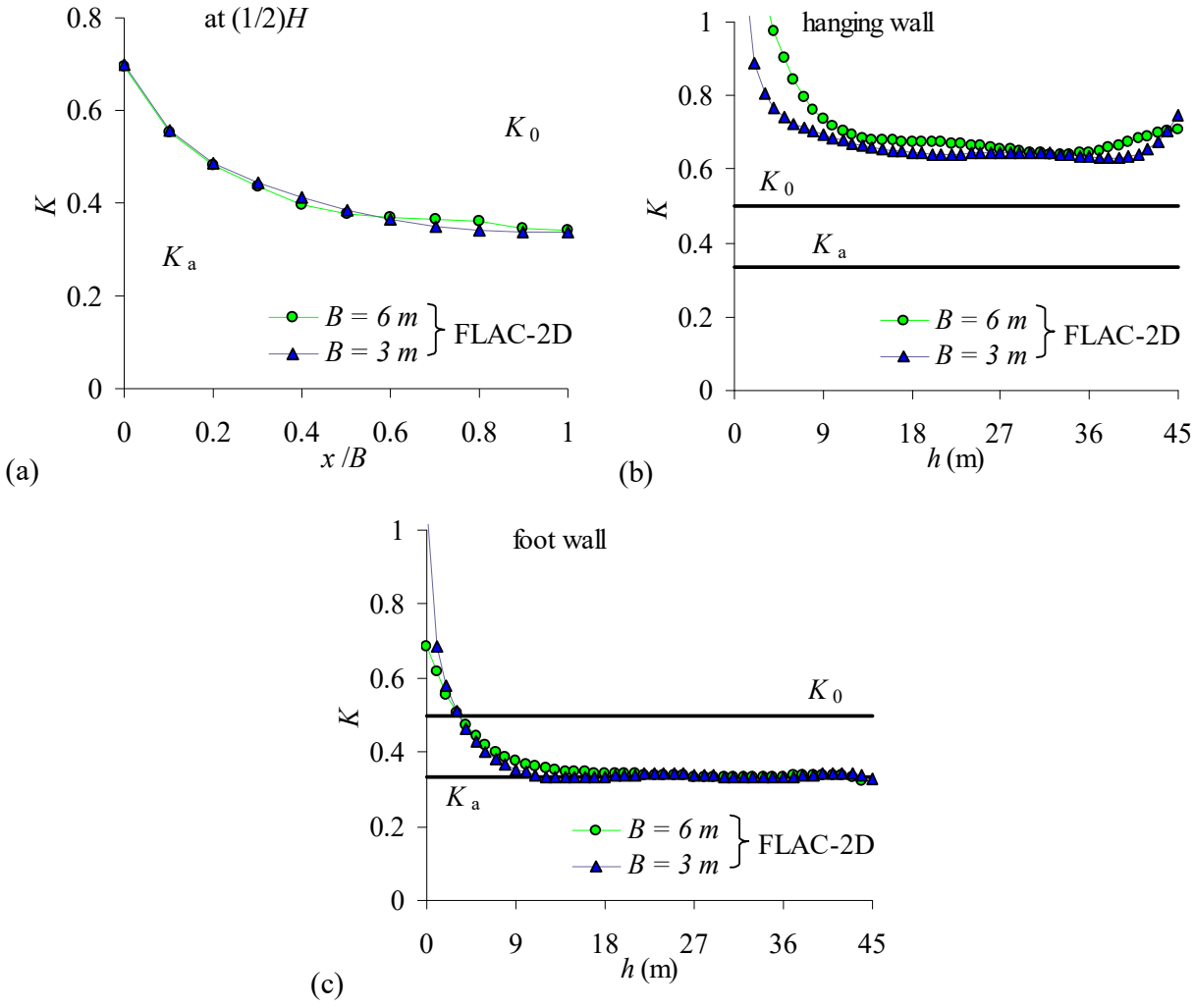

Fig. 6 shows that when E becomes higher than about 300 MPa, the stress distribution becomes oscillatory. This pattern has not been seen in previous simulations.

Fig. 7 also shows that the vertical stress in the stope is very sensitive to a variation of Poisson's ratio, while the horizontal stress is less sensitive to this factor. In general, an increase of Poisson's ratio tends to increase the horizontal stress and to reduce the vertical stress magnitude. The same observations were made previously (Li et al. 2007). It is thus deemed important to include a realistic value of Poisson's ratio in backfilled stope analysis. The stress distributions obtained here, with the multi-step filling simulation, is somewhat irregular (oscillatory), compared to those obtained with the pseudo-static (single layer) method (Li et al. 2007).

Figure 19. Variation of earth pressure coefficient K for different Poisson's ratio μ: (a) at mid-height of the stope, (b) along hanging wall, (c) along foot wall; other backfill properties are given in Table 1 (for α = 75°).

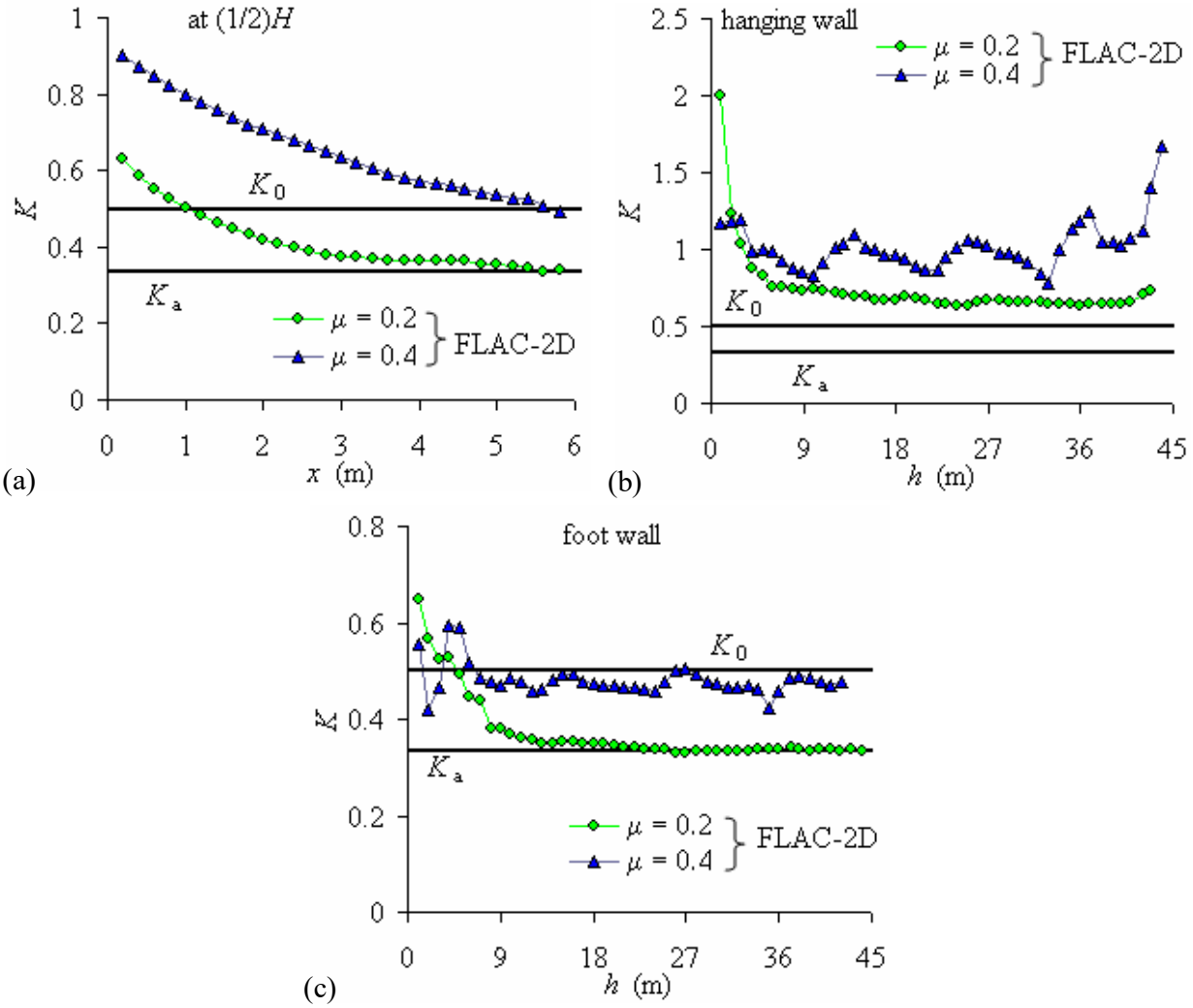

When the friction angle increases, the pseudo-static simulation approach (Li et al. 2007) indicates that the vertical stress decreases with an increase of friction angle from 10° to 40°. Results shown in Figure 8, however, indicate that the vertical stress becomes almost insensitive to a change in the friction angle for $\phi' \geq 20°$ (see Fig. 8). This observation better corresponds to the analytical solutions previously developed by the authors (Aubertin et al. 2003; Li et al. 2005a).

As for the effect of cohesion, the results shown here indicate that it is limited to a range of c' values between 1 kPa and about 50 kPa (Fig. 9). Figure 9 also shows that the stress distributions become wavy with depth when the cohesion is 10 kPa or higher. This indicates a change in the mechanical response of the backfill, from that of a particulate (granular) material to that of a cohesive medium where each

layer reacts somewhat like a beam. This behavior has not been reported in the literature (to the authors' knowledge), and will deserve further investigation.

Figure 20. Variation of earth pressure coefficient K for different backfill dilatation angle ψ': (a) at mid-height of the stope, (b) along hanging wall, (c) along foot wall; other backfill properties are given in Table 1 (for α = 75°).

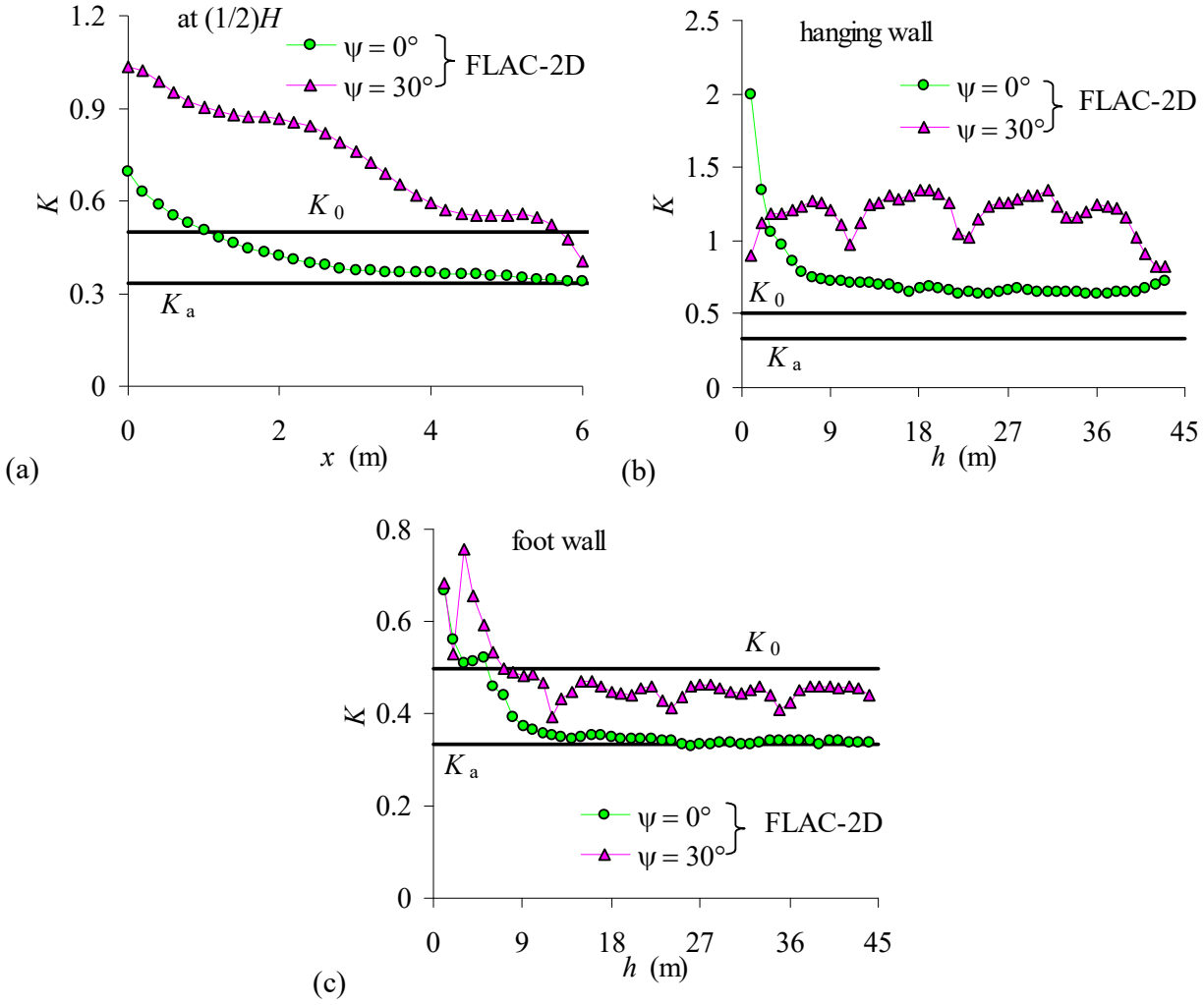

Finally, results shown above and in Li et al. (2007) indicate that the dilatation angle ψ' of the backfill also influences the stress distribution. There are, however, differences between the one-step pseudo-static method (Li et al. 2007) and the multi-step filling simulation used here. For instance, the former gives horizontal and vertical stresses that are almost insensitive to the variation of the dilatation angle ψ' between 5° and 30° while the latter results show that both stresses change when with dilatation

angle from 5° to 30°. The stress distribution also becomes wavy (oscillatory) with depth using multi-steps simulations (Fig. 10).

These results show that the adopted modeling approach (with FLAC-2D) may have a significant influence on the local stress values, and on the overall stress distribution.

Figure 21. Variation of earth pressure coefficient K for different backfill cohesion c': (a) at mid-height of the stope, (b) along hanging wall, (c) along foot wall; other backfill properties are given in Table 1 (for $\alpha = 75°$; K_0 and K_a calculated for $c' = 0$).

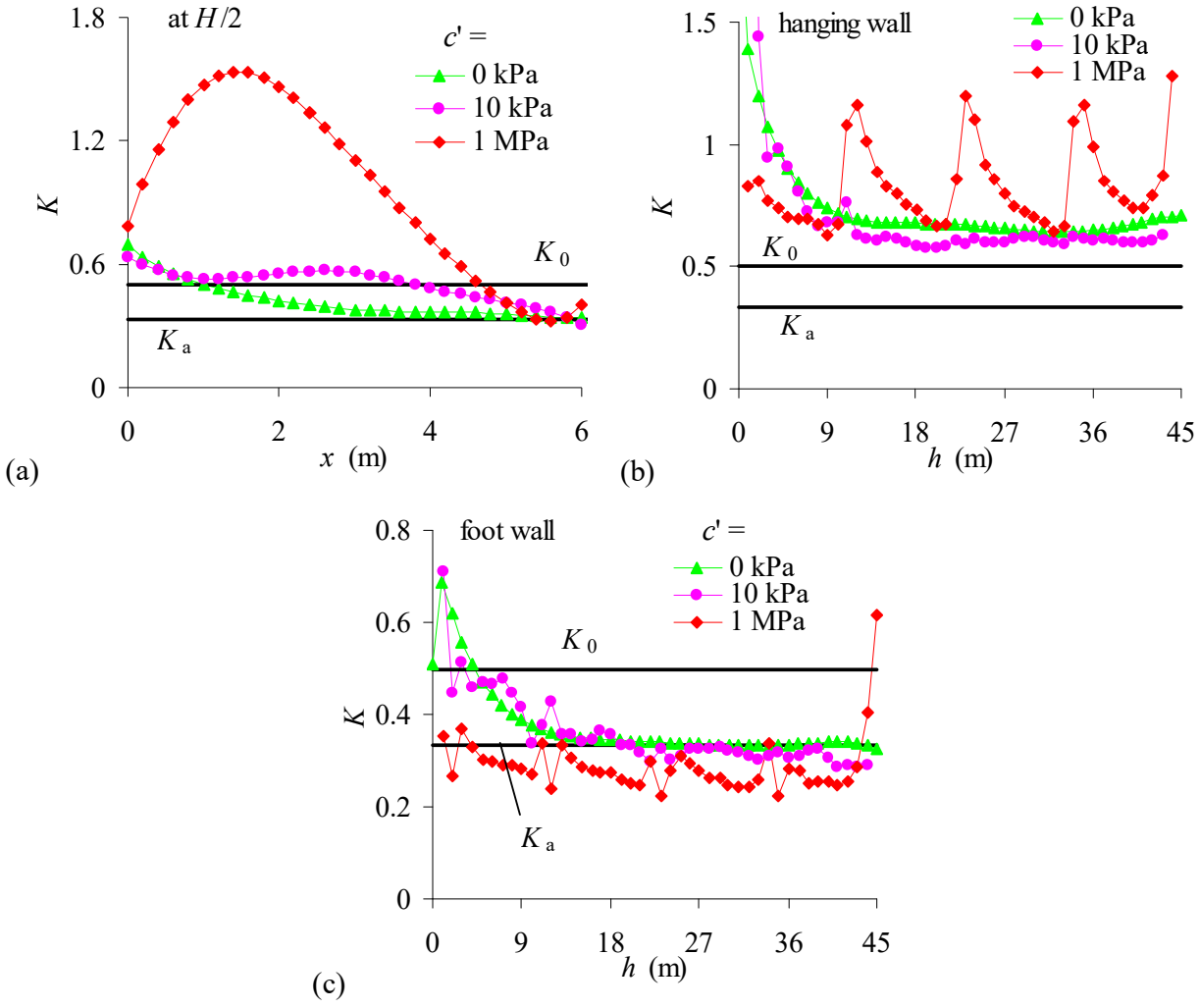

4.6 Earth reaction coefficient

The factor K (= σ_h'/σ_v'; σ_h' and σ_v' represent horizontal and vertical effective stresses when the backfill is saturated), known as the earth pressure coefficient, is a key component of most analytical solutions

developed to evaluate pressures on walls. These solutions typically use a constant K value over the entire height for calculating the stresses on retaining walls and in openings (e.g., McCarthy 1988; Aubertin et al. 2003; Brachman and Krushelnitzky 2005; Li et al. 2005a). Numerical simulations are used here to evaluate the earth pressure coefficients in backfilled stopes. These are compared with coefficients typically introduced in analytical solutions, which correspond to either at rest (K_0 = 1 - sinϕ', for $c' \cong 0$), or active ($K_a = (1-\sin\phi')/(1+\sin\phi')$); passive conditions ($K_p$) are not shown here because these are less relevant to the problems at hand. It can be seen (in Fig. 17) that the earth pressure coefficient value for vertical stopes ($\alpha = 90°$) is relatively constant along the stope width and height. This confirms that the assumption of a constant earth pressure coefficient within a vertical backfilled stope is reasonable. Figure 17 also shows that the earth pressure coefficient K for vertical stopes is fairly close to the active coefficient K_a, hence supporting the value of K which has been used in recently developed analytical solutions (Li et al. 2005a; Li and Aubertin 2008a). For inclined stopes, Figure 17 shows that the earth pressure coefficients along the foot wall and hanging wall are also fairly constant (for $\alpha = 60°$), as was postulated by Michalowski (1983) (for hoppers). However, the figure indicates that the earth pressure coefficient across the width of an inclined stope is not a constant, as it decreases gradually from the hanging wall to the foot wall. Thus, the value of K cannot be considered independent of the position along the width of the opening in this type of situation; analytical solutions developed for inclined stopes (Aubertin et al. 2005) should thus be modified to take this into account.

Figure 18 shows that the earth pressure coefficient K is not sensitive to the stope width B. For significantly inclined stopes (about $\alpha \leq 75°$), the earth pressure coefficient is seen to vary across the width and also along the stope height. The main variation occurs near the top of the stope (Fig. 18b, c).

Figures 19 and 20 show that the K value may also depend on Poisson's ratio μ (Fig. 19) and dilatation angle ψ' (Fig. 20). An increase of ψ' or μ tends to increase the earth pressure coefficient. These observations are not unexpected as it was seen above that these parameters also affect the mechanical response of the fill (see Figs. 7 and 10). For a given μ or ψ', the earth pressure coefficient varies across the width of the stope, but its value is relatively constant with depth. The results show that when the value of μ or ψ' is low, K_0 is a more representative estimate of the value of K near the hanging wall while K_a becomes a more adequate representation of K near the foot wall.

As can be expected, changing the backfill cohesion c' affects the value of K (Fig. 21). Although the earth pressure coefficient does not change significantly when c' is small ($c' < 10$ kPa), when the cohesion value becomes larger, the overall mechanical response of the fill changes (see Fig. 9) which

affects the K value. The earth pressure coefficient changes across the width of the stope and with depth. The K values can then differ significantly from those estimated for K_0 or K_a (with $c' = 0$). A constant earth pressure K is not a realistic assumption in this case.

4.7 Final remarks

The results obtained with FLAC-2D are only applicable to cases where the stope has a length that is much greater than its width (i.e. plane strain conditions). Otherwise, the effect of the third dimension has to been taken into account. Although analytical solutions have been developed for this purpose (Li et al. 2005a), more work is needed on the numerical analyses of inclined stopes in 3D.

Another limitation of the cases investigated here relates to the use of the Coulomb criterion. It is well known that this linear yield function is not always appropriate when dealing with frictional porous media, so another (more general) criterion may sometimes be preferable, particularly when dealing with tensile stresses or with relatively high mean pressures. In this regard, the authors have developed the multiaxial $MSDP_u$ criterion (e.g., Li et al. 2005b). Development of a related 3D elastoplastic model is underway and will be considered in additional analyses.

Some of the other factors neglected here may sometimes need to be taken into account when making a detailed analysis of backfilled stopes. These include pore water pressure and drainage, consolidation and settlement, suction induced strength gain (under unsaturated conditions), and evolution of the backfill strength during curing. These features are being addressed in complementary investigations conducted by the authors and collaborators (e.g., Godbout et al. 2004, 2007; Belem et al. 2007; Li and Aubertin 2008b).

5. CONCLUSION

This paper presents the main results of an extensive numerical investigation that illustrates the influence of stope geometry (inclination and width), backfill properties, and filling sequence. The results indicate that the stope inclination angle α has relatively little effect on the horizontal stress, while the vertical stress decreases significantly along the hanging wall and inclined central line when α is increased. Along the foot wall, the horizontal stress tends to decrease with the stope inclination, but the tendency for the vertical stress is not as well defined. The numerical simulations also confirm that neglecting the backfill deformability (modulus E) in limit equilibrium analyses is an acceptable simplification provided the value is not too large. The backfill Poisson's ratio, dilatation angle, and

strength parameters (ϕ', c') can, however, have a significant effect on the stress distribution. Nonetheless, the stress distribution may become insensitive to the cohesion value when it is very small ($c' < 10$ kPa) or very large ($c' > 50$ kPa, for the case investigated here). As for the filling sequence, the stress distribution appears to become insensitive when the number of layers exceeds a certain value, at least when the backfill is non-dilatant and cohesionless. Otherwise, the mechanical response of backfill may be highly dependent of the number of steps used to fill the opening. The results also show a behavior that may change from that of a particulate material to that of a consolidated material where each fill layer responds like a flexing beam. In the latter cases, multi-step simulations based on actual filling sequence and geometry should be considered to obtain representative results of the stress distribution. The evolution of the backfill strength during curing then becomes another factor to take into account (but not introduced in the analyses presented here).

ACKNOWLEDGEMENT

The authors acknowledge the financial support from the Institut de recherche Robert-Sauvé en santé et en sécurité du travail du Québec (IRSST), from NSERC and from partners of the Industrial NSERC Polytechnique-UQAT Chair on Environment and Mine Wastes Management (http://www.polymtl.ca/enviro-geremi/). The authors thank Dr. J. Molson for his review of the report.

REFERENCES

Andrieux, P., Brummer, R., Detournay, C., Hart, R. (eds.) 2003. FLAC and Numerical Modeling in Geomechanics - 2003. Proceedings of the Third International FLAC Symposium, Sudbury, Ontario, 21-24 October 2003. Taylor & Francis.

Aubertin, M. 1999. Application de la mécanique des sols pour l'analyse du comportement des remblais miniers souterrains. Short Course (Lecture Notes), 14^{e} Colloque en Contrôle de Terrain, Val-d'Or, 23-24 mars 1999. Association Minière du Québec.

Aubertin, M., Bussière, B., Bernier, L. 2002. Environnement et gestion des rejets miniers. Manual on CD-ROM, Presses Internationales Polytechniques.

Aubertin, M., Li, L., Arnoldi, S., Belem, T., Bussière, B., Benzaazoua, M., Simon, R. 2003. Interaction between backfill and rock mass in narrow stopes. In: Culligan PJ, Einstein HH, Whittle AJ (eds) Soil and Rock America 2003, Verlag Glückauf Essen (VGE), vol. 1, pp. 1157-1164.

Aubertin, M., Li, L., Belem, T., Simon, R., Harvey, A., James, M., Benzaazoua, M., Bussière, B. 2005. Méthodes d'estimation des pressions induites dans les chantiers remblayés. Symposium Rouyn-Noranda: L'Environnement et les Mines, 15-18 mai 2005, Rouyn-Noranda, Canada, CIM.

Belem, T., Benzaazoua, M., Bussière, B. 2000. Mechanical behaviour of cemented paste backfill, Proceedings of 53th Canadian Geotechnical Conference, 15-18 October 2000, Montréal, vol. 1, pp. 373-380.

Belem, T., Benzaazoua, M., Bussière, B., and Dagenais, A.-M. 2002. Effects of settlement and drainage on strength development within mine paste backfill. Tailings and Mine Waste'02, 27-30 January 2002, Fort Collins, Colorado. Balkema: Rotterdam, pp. 139-148.

Belem, T., Harvey, A., Simon, R., Aubertin, M. 2004. Measurement and prediction of internal stresses in an underground opening due to backfilling with cemented paste. Proceedings of the 15th International Symposium on Ground Support in Mining and Underground Construction: Ground Support 2004, 28-30 September 2004, Perth, Western Australia.

Belem, T., El Aatar, O., Benzaazoua, M., Bussière, B., Yilmaz, E. 2007. Hydro-geotechnical and geochemical characterization of column consolidated cemented paste backfill. Proceedings of the 9th International Symposium in Mining with Backfill, April 29-May 2, 2007, Montreal, Qc. CIM, CD-ROM.

Benzaazoua, M., Bussière, B., Aubertin, M., Ouellet, S., Godbout, J., Fiset, J.-F., Fall, M., and Belem, T. 2005. Contribution à l'évaluation du comportement environnemental des remblais miniers cimentés en pâte. Symposium Rouyn-Noranda: L'Environnement et les Mines, 15-18 mai 2005. CIM.

Billaux, D., Detournay, C., Hart, R., Rachez, X. (eds.) 2001. FLAC and Numerical Modeling in Geomechanics - 2001. Proceedings of the Second International FLAC Symposium, Lyon, France, 29-31 October 2001. Taylor & Francis.

Blight, G.E. 1986. Pressure exerted by materials stored in silos. Part I: coarse materials. Géotechnique 36(1): 33-46.

Brachman, R.W.I., Krushelnitzky, R.P. 2005. Response of a landfill drainage pipe buried in a trench. Canadian Geotechnical Journal, **42**: 752–762.

Cowin, S.C. 1977. The theory of static loads in bins. J. Appl. Mech. 44: 409-412.

Cowling, R. 1998. Twenty-five years of mine filling: Development and directions. Australasian Institute of Mining and Metallurgy Publication Series, No. 1, Proceedings of the 6th International Symposium on Mining with Backfill, April 14-16, 1998, Brisbane, Aust.

Detournay, C., Hart, R. (eds.) 1999. FLAC and Numerical Modeling in Geomechanics. Proceedings of the International FLAC Symposium, Minneapolis, Minnesota, 1-3 September 1999. Taylor & Francis.

Drescher, A. 1991. Analytical methods in bin-load analysis. Elsevier, New York.

Filz, G. M. 1996. Consolidation stresses in soil-bentonite backfilled trenches. Proc., 2nd Int. Congress on Environmental Geotechnics, Osaka, Japan, pp. 497–502.

Godbout, J., Bussière, B., Aubertin, M., Belem, T., Benzaazoua, M. 2004. Évolution des propriétés de rétention d'eau des remblais miniers cimentés en pâte durant le curage. Proceedings of the 57th Canadian Geotechnical Conference and the 5th joint CGS-IAH Conference, 24-27 October 2004, Quebec city, Session 4G, pp. 15-22.

Godbout, J., Bussière, B., Aubertin, M., Belem, T. 2007. Evolution of cemented past backfill saturated hydraulic conductivity at early curing time. Diamond Jubilee Canadian Geotechnical Conference and the 8th Joint CGS/IAH-CNC Groundwater Conference, 21-24 October 2007, Ottawa.

Handy, R.L. 1985 Arch in soil arching. Journal of Geotechnical Engineering 111(3): 302-318.

Handy, R.L. 2004. Anatomy of an error. Journal of Geotechnical and Geoenvironmental Engineering 130(7): 768-771.

Hassani, F., Archibald, J.F. 1998. Mine backfill. CIM, CD-ROM.

Hustrulid, W., Qianyuan, Y., Krauland, N. 1989. Modeling of cut-and-fill mining systems – Näsliden revisited. In: Hassani FP, Scoble MJ, Yu TR (eds) Innovation in Mining Backfill Technology, Balkema, pp. 147-164.

Itasca (2002) FLAC - Fast Lagrangian Analysis of Continua, User's Guide. Minneapolis, Itasca Consulting Group, Inc.

Kamon, M., Katsumi, T., Inui, T., Ogawa, Y., Araki, S. 2006. Hydraulic performance of soil-bentonite mixture barrier. Opportunities, Challenges and Responsibilities for Environmental Geotechnics - International Society of Soil Mechanics and Geotechnical Engineering's (ISSMGE) 5th International Congress, pp. 733-740. June 26-30, 2006, Cardiff, Wales, UK. Thomas Telford Services Ltd, London.

Kang, J., Parker, F., Yoo, C.H. 2007. Soil-structure interaction and imperfect trench installations for deeply buried concrete pipes. Journal of Geotechnical and Geoenvironmental Engineering 133(3): 277-285.

Knutsson, S. 1981. "Stresses in the hydraulic backfill from analytical calculations and in-situ measurements." Proceedings of the Conference on the Application of Rock Mechanics to Cut and Fill Mining, O. Stephansson, and M.J. Jones (eds.). Institution of Mining and Metallurgy, London, pp. 261-268.

Krynine, D.P. 1945. Discussion of "Stability and stiffness of cellular cofferdams" by Karl Terzaghi. Trans. Am. Soc. Civ. Eng. 110: 1175–1178.

Li, L., Aubertin, M. 2008a. An improved analytical solution to estimate the stress state in sub-vertical backfilled stopes. Canadian Geotechnical Journal (revised manuscript under evaluation).

Li, L., Aubertin, M. 2008b. Influence of water pressure on the stress state in stopes with cohesionless backfill Geotechnical and Geological Engineering (accepted).

Li, L., Aubertin, M., Simon, R., Bussière, B., Belem, T. 2003. Modeling arching effects in narrow backfilled stopes with FLAC. In: Brummer R, Andrieux P, Detournay C, Hart R (eds) FLAC and Numerical Modeling in Geomechanics – 2003, Balkema, pp. 211-219.

Li, L., Aubertin, M., Belem, T. 2005a. Formulation of a three dimensional analytical solution to evaluate stress in backfilled vertical narrow openings. Canadian Geotechnical Journal 42(6): 1705-1717 (with Erratum 43(3): 338-339).

Li, L., Aubertin, M., Simon, R., Bussière, B. 2005b. Formulation and application of a general inelastic locus for geomaterials with variable porosity. Canadian Geotechnical Journal 42(2): 601–623.

Li, L., Aubertin, M., Shirazi, A., Belem, T., Simon, R. 2007. Stress distribution in inclined backfilled stopes. Proceedings of the 9th International Symposium in Mining with Backfill, April 29-May 2, 2007, Montreal, Quebec, Canada. Canadian Institute of Mining, Metallurgy and Petroleum (CIM).

McCarthy, D.F. (1988) Essentials of soil mechanics and foundations: Basic geotechnics. Prentice Hall.

Michalowski, R.L. 1983. Approximate theory of loads in plane asymmetrical converging hoppers. Powder Technology 36(1):5-11.

Mitchell, R.J. 1992. Centrifuge model studies of fill pressures on temporary bulkheads. CIM Bulletin 85(960): 48-54.

Pirapakaran, K., Sivakugan, N. 2007a. A laboratory model to study arching within a hydraulic fill stope. Geotechnical Testing Journal 30(6): 1-8.

Pirapakaran, K., Sivakugan, N. 2007b. Arching within hydraulic fill stopes. Geotechnical and Geological Engineering 25(1): 25-35.

Spangler, M.G., Handy, R.L. (1984) Soil engineering. Harper and Row, New York, N.Y.

Take, W.A., Valsangkar, A.J. 2001. Earth pressures on unyielding retaining walls of narrow backfill width. Canadian Geotechnical Journal 38: 1220-1230.

Wang, Y.Z. 2000. Distribution of earth pressure on retaining wall. Géotech. 50(1), 83-88.

L'École Polytechnique se spécialise dans la formation d'ingénieurs et la recherche en ingénierie depuis 1873

École Polytechnique de Montréal

École affiliée à l'Université de Montréal

Campus de l'Université de Montréal
C.P. 6079, succ. Centre-ville
Montréal (Québec)
Canada H3C 3A7

www.polymtl.ca

ÉCOLE
POLYTECHNIQUE
MONTRÉAL